Ignitability of High-Fire-Point Liquid Spills

NP-1731
Research Project 1165-1

Final Report, March 1981

Prepared by

FACTORY MUTUAL RESEARCH CORPORATION
1151 Boston-Providence Turnpike
Norwood, Massachusetts 02062

Principal Investigator
A. T. Modak

Prepared for

Electric Power Research Institute
3412 Hillview Avenue
Palo Alto, California 94304

EPRI Project Manager
R. E. Swanson

System Performance Program
Nuclear Power Division

ORDERING INFORMATION

Requests for copies of this report should be directed to Research Reports Center (RRC), Box 50490, Palo Alto, CA 94303, (415) 965-4081. There is no charge for reports requested by EPRI member utilities and affiliates, contributing nonmembers, U.S. utility associations, U.S. government agencies (federal, state, and local), media, and foreign organizations with which EPRI has an information exchange agreement. On request, RRC will send a catalog of EPRI reports.

NOTICE

Prepared by
Factory Mutual Research Corporation
Norwood, Massachusetts

EPRI PERSPECTIVE

PROJECT DESCRIPTION

It is generally agreed that the major risk to electrical cables in a utility plant is the possibility of ignition by an external fire. The biggest potential offender in most accidental fire scenarios now being proposed is a spill of an ignitable fluid. In most cases the very conservative accident assumption has been that the fluid for some unexplained reason will immediately flash into flames with an immediate threat to any other flammable material in the room, such as electrical cable insulation. There is much evidence to indicate this is not probable with high-fire-point liquid spills. This project under RP1165-1 investigates high-fire-point liquids and reviews the immediate risk potential of such spills. The project does not negate the need for fire protection but rather tries to make the risk assumptions more realistic, which should make the fire protection design more applicable to the risk.

PROJECT OBJECTIVE

Previous fire prevention work had indicated that high-fire-point liquids are often very difficult to ignite and that a spill of liquid often made the fluid even more likely to be resistant to ignition. There was an indication that on very shallow spills, the surface, absorption, and heat transfer characteristics of the surface material also influenced the fire potential. This project exposed clean and contaminated flammable fluid material to varying radiant sources and looked at the effects of fluid depth and the underlying surface material and properties upon the fluid fire properties. Tests were planned on both a large scale and a small scale to verify the assumptions based upon small-scale results.

PROJECT RESULTS

Using floor materials modeled after those used by electric utilities, tests were run to determine the risks inherent in a spill of a flammable material. Factors identified as important in assessing the fire risk are discussed along with their relative importance. Volatile flammable material does represent a more immediate fire threat since it only needs an ignition source to become a flaming fire. At

the other end of the scale, high-fire-point fire-resistant fluids such as phosphate esters represent little risk. High-fire-point liquids require both a heat source to heat the fluid and a flame source. Since a 4-foot-diameter (1.4 meters) pool fire of burning gasoline with flames 7 to 10 feet in the air (2 to 3 meters) represents about 16 kW/m^2 heat flux to a nearby surface, the requirement of phosphate esters of over 16-minutes exposure to a 12 kW/m^2 heat flux before burning is impressive. With a heat flux of 12 kW/m^2, a major fire is already in progress, and fire fighting is already a requirement. The results of spill depth are also important. The project results indicate large spills should be confined because the greater surface area of a large spill is more risk than the depth. Small spills may be significantly more difficult to ignite if the spill is unconfined, especially if the floor surface also conducts heat away from the fluid. This report should be of interest to fire protection designers and engineering and operations departments.

Roy E. Swanson, Project Manager
Nuclear Power Division

ABSTRACT

This work identified the conditions under which a spill of flammable liquid on an ambient-temperature floor could represent a fire threat to grouped cables in an electric utility installation. Five high-fire-point, flammable, hydrocarbon liquids were tested in this program. They were: 1) #2 fuel oil; 2) #6 residual oil; 3) Mobil DTE 797 turbine lubricating oil; 4) Pennzoil 30-HD motor oil; and 5) Fyrquel 220 hydraulic control fluid. Three floor materials were tested: 1) float-finished (21 MPa) concrete; 2) epoxy-coated (21 MPa) concrete; and 3) steel. The fire hazard presented by a spill depends on five factors: 1) spill depth; 2) thermal inertia of the floor under the spill; 3) fire point of the flammable liquid spill; 4) thermal energy available to heat the spill to its fire point; and 5) the availability of an ignition source to ignite the spill after reaching fire point. The relative importance of each factor is identified.

ACKNOWLEDGMENTS

The author would like to thank J. de Ris, R.A. Hemstreet, G. Heskestad, G.H. Markstein and L. Orloff for helpful discussions during the course of this work; and J. Polo for his help in conducting the experiments. The problem of analyzing a finite depth, flammable liquid spill on a conducting substrate was first suggested to this author by R. Friedman.

The large-scale experiments reported in Section 2 were supervised by J.P. Hill.

The experiments reported in Section 2.2 were suggested by Mr. Roy E. Swanson (Project Manager, Nuclear Power Division, Electric Power Research Institute) during an interim program review.

CONTENTS

Section		Page
1	INTRODUCTION	1-1
2	LARGE-SCALE EXPERIMENTS	2-1
	2.1 Large-Scale Test Using A Heptane Pool Fire	2-1
	2.2 Deep Pools of Hydrocarbon Liquids Exposed to Weld Spatter Or Oxyacetylene Torch	2-4
	2.3 Shallow Pools Of Hydrocarbon Liquids Exposed To Weld Spatter Or Oxyacetylene Torch	2-5
3	SMALL-SCALE EXPERIMENTS	3-1
	3.1 Simulation Of Radiant Flux From A Source Fire	3-1
	3.2 Simulation Of Floor Materials In Utility Installations	3-3
	3.3 Thermal Properties Of Hydrocarbon Liquids	3-5
	3.4 Infrared Absorption And Transmission In Hydrocarbon Liquids	3-11
	3.5 Surface Temperatures For Deep Spills Of Hydrocarbon Liquids	3-15
	3.6 Depths Of Unconfined Spills	3-15
	3.7 Surface Temperatures Of Unconfined Spills	3-19
	3.8 Definition Of Ignition Time	3-22
4	THEORY	4-1
	4.1 Semi-Infinite Pools Of Hydrocarbon Liquids	4-2
	4.2 Spills Of Finite Depth	4-8
5	CONCLUDING REMARKS	5-1
REFERENCES		6-1
APPENDIX A	EFFECT OF THERMOCOUPLE SIZE ON SURFACE TEMPERATURE MEASUREMENTS	A-1
APPENDIX B	SOLUTION OF EQUATIONS 4-6 AND 4-7 BY LAPLACE TRANSFORMS	B-1

ILLUSTRATIONS

Figure		Page
1-1	Schematic Of A Source Fire And A Flammable Liquid Spill On A Concrete Substrate	1-3
2-1	Schematic Of A Large-Scale Experiment Using A Heptane Source Fire of Diameter 1.2 m	2-3
3-1	Schematic Of A Small-Scale Experiment Showing Radiant Heater Assembly	3-2
3-2	Normalized Flux Distribution For 2 Voltage Settings Of The Tungsten-Quartz Radiant Heater	3-4
3-3	Thermal Conductivities Of Hydrocarbon Liquids Are Shown As A Function Of Temperature (300 To 600 K) Parametric In API Degrees	3-7
3-4	Densities Of Hydrocarbon Liquids Are Shown To Decrease With Temperature (300 To 600 K)	3-8
3-5	Specific Heats Of Hydrocarbon Liquids Are Shown To Increase With Temperature (300 To 600 K)	3-9
3-6	Volumetric Heat Capacities (i.e., Product Of Density And Specific Heat) Of Hydrocarbon Liquids Are Shown As A Function Of Temperature (300 To 600 K) Parametric In API Degrees	3-10
3-7	Measured Surface Temperature Rise Above Ambient For A 120 mm Deep Pool Of Pennzoil 30-HD Is Shown As A Function Of Time Of Exposure To 13.8 kW/m^2 Radiant Flux	3-12
3-8	Measured Transmittance, τ, To Thermal Radiation From The Tungsten-Quartz Lamps Is Shown As A Function Of Liquid Depths For 4 Hydrocarbon Liquids And For Liquid H_2O	3-14
3-9a	Experimental Measurements Of Surface Temperature Rise Above Ambient Are Shown For 4 Hydrocarbon Liquids As A Function Of Time Of Exposure To 13.8 kW/m^2 Radiant Flux	3-17
3-9b	26 kW/m^2 Radiant Flux	3-17
3-10	Measured Spill Areas Are Shown As A Function Of Spill Volume For An Unconfined Spill Of Pennzoil 30-HD On Three Horizontal Surfaces: 1) Steel; 2) Epoxy-Coated Concrete; and 3) Uncoated Concrete	3-18
3-11a	Measured Surface Temperature Rise Above Ambient Is Shown As A Function Of Time Of Exposure To 13.8 kW/m^2 Radiant Flux, For Unconfined Spills Of Four Oils On An Epoxy-Coated Concrete Substrate	3-20
3-11b	Temperature Response Of Unconfined Spills On A Steel Substrate For Four Hydrocarbon Liquids	3-23
3-12	Measured Surface Temperature Rise Above Ambient Is Shown As A Function of Time Of Exposure To 26 kW/m^2 Radiant Flux For Unconfined Spills Of Fyrquel 220 On 1) Epoxy-Coated Concrete And 2) Steel	3-24

Figure		Page
4-1	Measured Surface Temperature Of An Opaque (Pennzoil 30-HD With 10 Percent By Volume Lampblack Mixture Added), Semi-Infinite (120 mm Deep), Medium Is Compared With Theory (Eq. 4-5) Using Three Different Values Of Net Flux $\dot{q}''$ = 13.8, 8.9 And 6.8 kW/m^2	4-4
4-2a	Measured Surface Temperatures (Shaded Region) Of Four Semi-Transparent, Semi-Infinite, Hydrocarbon Liquids Are Compared With Theory (Eq. 4-4) Using A Net Flux $\dot{q}''$ = 10 kW/m^2 For An External Flux Of 13.8 kW/m^2 From The Tungsten-Quartz Lamps	4-6
4-2b	Comparison Of Theory (Solid Line) And Experiment (Shaded Region) For 26 kW/m^2 External Flux	4-7
4-3	Schematic Of A One-Dimensional System Showing An Opaque, Finite Depth Spill On A Semi-Infinite Substrate	4-9
4-4	Measured (Heavy Line) Surface Temperature Of A (99.9 Percent Purity) Copper Cylinder Of Finite Depth (103 mm) Is Compared With The Finite Depth Theory of Eq. (4-15) Using $\dot{q}''$ = 20.2 kW/m^2	4-12
4-5a	A Comparison Of Experiment (Solid Line) And The Range (Shaded Region) Predicted By Two Theoretical Limits (Opaque Limit - Eq. 4-15; And Fully Transparent Limit - Eq. 4-22) For An Unconfined Spill Of Pennzoil 30-HD On A Steel Substrate	4-15
4-5b	Unconfined Spill Of Pennzoil 30-HD On An Epoxy-Coated Concrete Substrate	4-17
5-1	Thermal Radiation Flux From A Typical Hydrocarbon Source Fire To A Spill Noncontiguous With The Fire But Adjacent To It Is Shown As A Function Of Source Fire Diameter	5-2
5-2	Ignition Time (Piloted) For Deep Spills Of Semi-Transparent Hydrocarbon Liquids Are Shown As A Function Of The Net Radiant Flux To The Spill For A High Fire Point Liquid (586 K, Fyrquel 220) And A Relatively Low Fire Point Liquid (402 K, #2 Fuel Oil)	5-3
A-1	Measured Surface Temperature Rise Above Ambient Versus Time Of Exposure To 13.8 kW/m^2 Radiant Flux For A 120 mm Deep Pool Of Pennzoil With 20 Percent Lampblack Mixture Added	A-2

TABLES

Table		Page
2-1	Critical Fire Temperatures For Hydrocarbon Liquids And Ignition Times For Deep Pools Exposed To A 1.2-m Diam Heptane Pool Fire	2-2
3-1	Mean Thermal Properties Of Concrete, Copper And Steel	3-6
3-2	Specific Gravities And API Degrees For Hydrocarbon Liquids	3-6
3-3	Properties Of Hydrocarbon Liquids	3-16
3-4	Unconfined Spill Depths For Hydrocarbon Liquids On Epoxy-Coated Concrete And Steel	3-21
3-5	Comparison Of Times To Ignition And Fire Point	3-21

NOMENCLATURE

$c_{1,2}$	specific heat of flammable liquid or substrate, (J/g•K)
d	depth of liquid, mm
G	specific gravity of hydrocarbon liquids
k	gray absorption coefficient of hydrocarbon liquids, m^{-1}
m	$(\lambda_2\rho_2c_2/\lambda_1\rho_1c_1)^{1/2}$ root of thermal inertia ratio
n	index of summation
$\dot{q}''$	external flux, kW/m^2
s	Laplace transformed parameter for time
ΔT	surface temperature rise above ambient, K
$T_{1,2}$	temperature, K
t	time, s
x	distance, m
$\alpha_{1,2}$	$\lambda_{1,2}/(\rho_{1,2}c_{1,2})$ thermal diffusivity of flammable liquid or substrate, m^2/s
$1-\gamma$	surface absorptivity of hydrocarbon liquid
$\lambda_{1,2}$	thermal conductivity of liquid or substrate, W/(m•K)
θ	temperature rise above initial temperature, K
$\rho_{1,2}$	density of liquid or substrate, g/m^3
σ	(1-m)/(1+m), or Stefan-Boltzmann constant
τ	transmittance of hydrocarbon liquids

Superscripts

-	Laplace transformed variable
.	per unit time, s^{-1}
"	per unit area, m^{-2}

Subscripts

0	initial condition at time t=0
1	liquid
2	substrate

SUMMARY

S.1 PROGRAM DESCRIPTION

This project was initiated to better understand the fire risks of flammable fluid spills. The presence of flammable materials in an area always is an increased risk to that area. This program is specifically concerned with the risk to grouped cables caused by a flammable liquid spill, but the risk could be to any heat sensitive equipment or structures.

A fire from a spilled flammable liquid could ignite grouped cables and spread through the cable assembly. The fire could cause localized damage to cables by flame radiation or by direct impingement of hot combustion products in the fire plume. Failure could occur in cables resistant to ignition even if self-propagating flame spread did not occur.

It has been common practice to make the conservative assumption that a flammable liquid spill is, by virtue of its existence, an immediate fire hazard. It has been assumed that such a spill is a fully developed fire. This assumption asserts that a highly volatile flammable cleaning fluid (alcohol) and a high fire point lubricating oil present the same degree of fire hazard. The cleaning fluid is certainly a more immediate fire threat being subject to ignition by the smallest spark. The fire points of such liquids are less than the ambient temperatures normally encountered in an utility. On the other hand, some high fire point lubricating and hydraulic fluids in thin layers ((~1 mm) on concrete or steel substrates (floors)) would require sustained heat fluxes (of the order of 20 kW/m^2) to cause the liquid surface to reach the fire point. However, the requirement of a heat source capable of delivering 20 kW/m^2 to the liquid spill surface implies the presence of a substantial fire independent of the spill.

The assumption of a spill automatically becoming a fire has been relaxed in the present program. Here, it is not necessarily accepted that every spill ignites and results in a fire. Whether or not a spill ignites depends on several factors: 1) depth of spill; 2) thermal properties of the floor under the spill; 3) fire point of the liquid spilled; 4) thermal energy available to heat the liquid to its

fire point; and 5) availability of an ignition source (e.g., a pilot flame or welding sparks) to ignite the spill once its surface has been raised to its fire point.

A suitable mix of the above factors is necessary to ignite a flammable liquid spill. A quantitative understanding of this mix will be useful in evaluating flammable liquid spill scenarios to determine whether such spills represent fire hazards. In those cases where it is determined that a fire hazard exists (ignition is likely) the results of a previous EPRI sponsored study* should be used to assess the threat to the particular utility location.

S.2 PROGRAM OBJECTIVE

The objective of the present program was to determine the conditions under which a spill of flammable liquid could represent a fire threat to grouped cables in an electric utility installation. The following five typical high fire point liquids were tested in large- as well as small-scale test configurations: 1) #2 fuel oil, 2) #6 residual oil, 3) Mobil DTE 797 turbine lubricating oil, 4) Pennzoil 30-HD motor oil, and 5) Fyrquel 220 hydraulic control fluid. Three floor materials were used in the present program: 1) float finished (21 MPa) concrete, 2) epoxy-coated concrete, and 3) steel.

Since full-scale tests are expensive and difficult to conduct in a sufficiently controlled manner, another objective of this program was to develop small-scale test methods and analytic formulae to determine the ignitability of liquid spills as a function of the important controlling parameters. Small-scale test results and calculations using the formulae were found to agree reasonably well with the large-scale tests.

The formulae developed in the program, in conjunction with a limited set of small-scale tests, could be used to provide a relatively inexpensive and rapid method for classifying the ignitability of flammable liquid spills in electric utility installations. Because there is but little empiricism in the formulae, extrapolations and generalizations are possible.

*"Assessment of Exposure Fire Hazards to Cable Trays," J.S. Newman and J.P. Hill, EPRI Research Project 1165-1-1, Technical Report, June 1980, FMRC J.I. 0C2R7.RC, RC80-T-56.

S.3 RESULTS AND CONCLUSIONS

Although this study has demonstrated that it is possible to relax the assumption that all spills of flammable liquids will result in fires, it cannot be categorically stated under all conditions that some fluids are safe and others are not. It is obvious that any fluid with a fire point near to or lower than ambient temperatures is a fire hazard and may be expected to ignite readily. This leaves for consideration those fluids with fire points above ambient temperatures which are the principal subject of this report.

In order to use the results of this report, it is necessary to employ a liquid spill scenario which may be expected to vary from location to location. The basic steps in this evaluation are given below and these will also serve to summarize the type of information contained in this report.

1. Identification Of The Flammable Liquid

A flammable fluid spill scenario requires the identification of the fluid involved as well as its basic physical and flammability properties. These are a) fire point, b) thermal conductivity, c) volumetric heat capacity and d) transparency to thermal radiation. In this report it is shown that the thermal conductivities and volumetric heat capacities for hydrocarbon fluids are nearly the same and, for most fluids, the values given in this report may be used. The fire point is an important parameter and must be known (or measured) for each fluid. Fire points from the ASTM D-92 Cleveland open cup method may be used.

Specification of the transparency of the fluid is troublesome. However, from a practical point of view this report has shown that most fluids can be considered as either semi-transparent or opaque. The semi-transparent fluids are those which are clean and free of obvious contamination. Opaque fluids generally are those which are contaminated and appear dark or even black. The ignition of these two cases is considered in this report. If there is uncertainty as to which case applies, the most conservative approach would be to treat the fluid as opaque.

The results of this report may be used directly for #2 fuel oil, #6 residual oil, Mobil DTE 797, Pennzoil 30-HD and Fyrquel 220 which were used in this study.

A description of the significance of the fluid parameters is given in Section 1. (pp. 1-2 to 1-4).

2. Identification Of Spill Surface (Floor) And Spill Depth

The thermal properties of the spill surface are important because the temperature response of the liquid surface (temperature rise under an external applied heat flux or ignition source) is dependent both on thermal properties (heat sink properties) of the floor and the thermal conductivity of the liquid layer. This report considers both steel and concrete floor materials. (The concrete surfaces studied were a) float finished (21 MPa) and b) epoxy-coated.) Under equivalent conditions the liquid surface temperature rise is more rapid with concrete than with a more highly conducting surface such as steel.

The liquid spill depth is also an important parameter since it controls the flow of heat from the liquid surface to the floor. It is this heat flow balance (external heat flux to the liquid surface and heat conduction through the liquid layer to the floor) which determines the rate of temperature rise of the liquid surface to the fire point.

In this report we consider unconfined and confined spills. An unconfined spill is one which spreads out to a depth which is determined primarily by the surface tension of the fluid. The depth of an unconfined spill on a truly horizontal floor is independent of spill volume and, if the floor is nonabsorbing (nonporous), is relatively independent of the floor material. Unconfined spill depths are generally less than 1 mm but will vary from liquid to liquid. These depths are easily measured with test spills on the floor material of interest.

The depth of a confined spill is dependent on the spill volume and the volume of the confinement which could be determined by the floor area of the room if the spill is large enough. If the spill depth is large enough, the rate of rise of the liquid surface temperature to the fire point will be determined solely by the properties of the liquid and external heat flux and will not be dependent on the thermal properties of the floor material. Since the thermal and absorption-transmission properties of the fluids used in this program were essentially the same, it is expected that the surface temperature response of all these materials will be the same when exposed to the same external radiation flux. This is demonstrated in Figure 3-9a.

3. Ignition Source

A high fire point liquid spill will not become a fire unless there is also present a heat source which will raise the liquid surface at least to the fire point temperature. Generally, this heat source will be a fire which pre-existed or occurred after the spill. In either case, this fire would occur independently of the spill.

In this report the ignition fire or external heat source is specified in terms of the radiant heat flux which the ignition fire could deliver to the liquid spill surface. As a reference point we note that a 1.2 m (4 ft) diam pool of burning heptane (similar to gasoline) would deliver a net* heat flux of about 16 kW/m^2 to the surface of an adjacent liquid spill. A 1.2 m diam pool fire is a formidable heat source consisting of flames extending 2 to 3 meters (7 to 10 ft) above the heptane surface. The heat fluxes from other size hydrocarbon sources are shown in Figure 5-1.

The following examples from the text illustrate the dependence of ignition time on the liquid spill fire point and size of the external heat source (fire). These results refer to semi-transparent deep spills where the thermal properties of the floor are not important:

1. At a net heat flux of 12 kW/m^2 (approximately 0.9 m diam heptane pool fire), it requires 1000 s (16.7 min) to ignite Fyrquel 220. When the net heat flux is 16 kW/m^2 (1.2 m diam heptane pool), the ignition time is 400 s (6.67 min).
2. At a heat flux of 12 kW/m^2 it requires 1000 s (16.7 min) to ignite Fyrquel 220 (fire point 586 K) but only 90 s (1.5 min) to ignite #2 fuel oil (fire point 402 K).
3. Figures 5-1 and 5-2 show that it takes a long time (>> 1000 s) to ignite deep, high fire point flammable liquid spills if the ignition source is less than 200 mm (7.9 in.) diam.
4. Under equivalent conditions, the ignition times for thin, unconfined spills will be much longer than quoted above.

4. Liquid Spill Scenario Evaluation

Once the essential parameters of a liquid spill scenario have been collected, the question becomes not whether ignition will occur, but how long will it take? If the ignition time is longer than the time for response and corrective action to the spill and ignition source, then the spill does not represent an additional hazard. Large ignition sources of the sizes quoted above would demand immediate action regardless of the additional presence of a liquid spill.

The estimation of ignition times of liquid spills can be made by reference to the following parts of this text:

*Net heat flux is the flux delivered by the 1.2 m diam heptane pool fire source less the heat loss from the spill surface by convective cooling of and reradiation from the spill surface.

1. Deep Spills

   •opaque spills (Eq. 4-5; also Figure 4-1)
   •semi-transparent spills (Eq. 4-4; also Figures 4-2a and 4-2b)

2. Shallow Spills

   •opaque spills (Eq. 4-15)
   •transparent spills (Eq. 4-22; also Figures 4-5a and 4-5b)

5. Relative Hazards Of Confined And Unconfined Spills

This report is concerned solely with requirements for ignition of liquid layers on heat conducting floors. It is shown clearly that thin layers are more difficult to ignite than thick layers. Thus, it would appear that, for a given liquid spill volume, it would be preferable to let the liquid spread out as much as possible. However, it was shown in Reference 1 that, once ignited, the heat release rate (fire intensity) increases as the burning surface area increases. Thus, once ignited it would be preferable to have the liquid confined to as small a surface area (deep pool) as possible to minimize the threat to the spill location.

The two desired conditions relating to fire hazard from ignition, and hazard from combustion after ignition are in direct contradiction. This situation can only be resolved by means of an analysis involving not only specification of the spill conditions, but also the effect that a pool fire would have on local equipment and structures. When only modest spill volumes are anticipated, one would most likely be concerned with ignition alone. For such a case, the thin layer analysis reported here should be used. When large volume spills are possible it is more likely that one would be dealing with thick layers. In this case, it would be preferable to install dykes to confine the fluid and, if possible, to supply drainage to a sump and/or perforated plates over the dyked area to allow access of the liquid, yet minimize heat transport and air access for combustion to the contained liquid. Neither of these alternatives have been investigated in this report, but they merit consideration.

Under no circumstances should the use of the results of this report imply that fire protection is not required in locations where flammable materials are present.

To summarize, the following noteworthy results (applicable to the fluids studied) emerge from this work:

1. Regardless of spill depth, it is very difficult to ignite a spill by less than 60-s exposure to weld spatter or less than 15-s direct exposure to a oxyacetylene welding torch.

2. It takes a long time (>>1000 s) to ignite a spill adjacent to a source fire if the source fire is less than 200 mm in diameter. For larger diameters, ignition times decrease rapidly with increasing fire size.

3. Infrared transmission and thermal properties of most hydrocarbon liquids are similar. Their fire points, however, can differ markedly.

4. Deep spills present a greater fire hazard than shallow spills; i.e., shallow (< 1 mm deep) spills on a concrete or steel floor do not present a fire hazard unless the thermal flux is very high (>20 kW/m^2).

5. Low-fire-point spills are more hazardous than high-fire-point spills.

6. For non-absorbing floors, the depth of an unconfined spill primarily depends on the surface tension of the liquid and not on the floor material. Unconfined spill depths on truly horizontal floors are independent of spill volume. Hydrocarbon liquid spills show markedly differing unconfined spill depths. These depths may vary by as much as a factor of 4 and are all generally less than 1 mm deep. Because of different depths, the surface temperature response of unconfined spills varies from liquid to liquid. The temperature response of a shallow spill depends on the thermal properties of the floor. For example, the temperature rise of an unconfined spill on a concrete substrate is more rapid than on a highly conducting substrate such as steel.

7. The ignition time of a spill can be estimated reasonably well on the basis of the time to reach its fire point. The simple formulae developed here can provide satisfactory estimates of ignition times for deep as well as shallow spills of flammable liquids.

Section 1
INTRODUCTION

The purpose of this work is to determine the conditions under which a spill of a flammable liquid with a fire point above ambient temperature could represent a fire threat to grouped cables in an electric utility installation. Liquid spills with fire points below ambient temperature (e.g., gasoline, ethyl alcohol, etc.) usually present a serious fire threat in an electric utility installation. It is obviously desirable to reduce the likelihood of such spills. The present work addresses the question of the fire hazard presented by a high-fire-point liquid spill on the ambient temperature floor of an electric utility installation.

Grouped cables in electric utility (1) installations are potentially subject to damage by fire. Fires in grouped cables or cable tray systems could cause loss of production, equipment damage and threat to personnel. The fire could originate in the cables themselves by means of overloading or short-circuiting or perhaps in combustible contaminants on the cables, e.g., dust, oil, etc. The ignition of combustible contaminants would require an external ignition source, e.g., welding sparks. Combustible contaminants are probably not a serious threat in a facility with good housekeeping. Further, it is generally very difficult to cause a sustained, spreading ignition of grouped cables by direct short-circuiting within a filled cable tray. A more serious threat to grouped cables is a fire originating external to the cables. Such a fire could originate in flammable debris or flammable liquids (cleaning fluids, lubricating fluids, etc.) which are accidentally spilled on the floor. An exposure fire could ignite the cables and subsequently, flames could spread through the cable installation. Or an exposure fire could cause localized damage due to flame radiation or by direct impingement of hot combustion products in the plume above the exposure fire. Damage and perhaps failure could occur in cables normally resistant to ignition, even if a self-propagating flame spread were not established in the affected cables.

It is common for regulatory agencies to propose fire scenarios in various utility operations. These agencies often require an estimate of potential damage that might occur in exposed cable trays. Frequently, it is assumed that a flammable liquid has been spilled on the floor (see Figure 1-1) under or near a set of cable

trays. It is also assumed that this liquid has been ignited, although usually no method of ignition is specified. The conservative assumption is often made that the pool of flammable liquid, regardless of its fire point or depth, will behave as if it were a fully developed fire.

The nature of the above assumption is investigated in greater detail in the present work. Here, it is not necessarily accepted that every spill automatically ignites and results in a fire.

The spill volume could vary from as little as one quart to perhaps as much as a 55-gal drum, depending on the kind of activity, location and administrative controls on the use of flammable liquids in the facility. If the spill is of limited volume, it is likely to spread out in a thin layer on a relatively cold, thermally massive floor of concrete, or perhaps steel. For ignition to occur in a high-fire-point liquid, it is essential that there be an ignition source available which can deliver thermal energy and raise the surface temperature of the liquid layer to its fire point. Highly volatile liquids will ignite at ambient temperatures. However, liquids with relatively high fire points spilled on a cold floor may not ignite at all or may take hours to ignite unless exposed to very high heat fluxes. It may be that very high heat fluxes are unlikely to occur in real life situations.

The present work specifically addresses the issue of ignitability. The ignitability of a particular liquid spill will depend on: 1) the properties of the liquid which determine the extent of spread and the resultant liquid pool thickness; 2) the flammability properties of the liquid which include its fire point and thermophysical properties governing the absorption and conduction of energy through the liquid layer to the floor; 3) the thermal properties of the floor which determine the extent to which the floor acts as a heat sink; and 4) the heat flux to the spill layer from the source (see Figure 1-1) fire. This heat flux is required to raise the liquid surface temperature to the fire point for ignition to occur.

The time required for ignition will be determined by a balance between the incoming heat flux and heat losses through the liquid layer to the underlying floor.

In this work, we have investigated the ignitability of five frequently used high-fire-point oils on three kinds of floor materials that might be encountered in a typical electric utility installation. The oils were: 1) #2 fuel oil; 2) #6 residual oil; 3) Mobil DTE 797, turbine lubricating oil; 4) Pennzoil 30-HD motor oil; and 5) Fyrquel 220 hydraulic control fluid. The three kinds of floors were:

1) 21 MPa - (uncoated) concrete with a float finish; 2) 21 MPa - concrete with a 0.4-mm thick protective coating of epoxy (Koppers Bitumastic No 300-M); and 3) AISI C 1018 Cold rolled steel floor. Several different experiments at large as well as at small scales were conducted. Critical parameters which control the ignitability of oil spills were identified and, finally, a simple theory for estimating the time to ignite an oil spill was developed. Experimental and theoretical results were noted to be in reasonable agreement.

The experiments are described in Sections 2 and 3. The theory is developed and compared with experimental results in Section 4. A summary of the results is provided in Section 5.

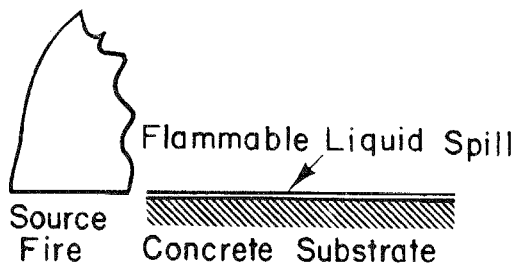

Figure 1-1. Schematic of a source fire and a flammable liquid spill on a concrete substrate.

Section 2
LARGE-SCALE EXPERIMENTS

Large- as well as small-scale experiments were conducted for studying the ignitibility of liquid spills. Large-scale experiments are described in the present section. Small-scale experiments are described in Section 3.

Three types of large-scale experiments were performed on five high-fire-point oils to simulate conditions that might occur in an electric utility installation. The first large-scale test was performed using a 1.2-m diam heptane source fire. The second and third large-scale tests were designed to determine the ignitibility of deep (50 mm) and shallow (4 mm) pools of oil or a concrete floor with the oil exposed to weld spatter or to a welding torch.

The three large-scale tests are described in Sections 2.1 to 2.3.

2.1 LARGE-SCALE TEST USING A HEPTANE POOL FIRE

This test simulated a situation where a (source) fire had already occurred in an electric utility installation. The source fire was assumed to have grown to a large enough size so that it threatened to ignite an accidental spill of oil on the floor. The volume of the oil spill was assumed to be large and confined and consequently the spill depth was large (depth = 50 mm). It was also assumed that the source fire was non-contiguous with, but adjacent to, the oil spill.

To simulate the above situation, a 1.2-m diam heptane pool was used as a source fire. The heptane pan was 83 mm deep and filled with heptane to a depth of 76 mm. Five nearly cylindrical (top diam 206 mm; bottom diam 187 mm, 156 mm deep) galvanized steel containers were packed with chunks of concrete debris up to a depth of 106 mm. The mean diameter of the debris was 25 mm. The debris approximately simulated a concrete floor. Each container was filled to the rim with oil so that a 50-mm layer of oil covered the debris. Table 2-1 lists the five oils used and their fire points. Figure 2-1 is a schematic of the heptane source fire and the location of the oil containers with respect to the source fire. The edges of the heptane pan and oil containers were 152 mm apart.

Table 2-1

CRITICAL FIRE TEMPERATURES FOR HYDROCARBON LIQUIDS AND IGNITION TIMES FOR DEEP POOLS EXPOSED TO A 1.2-m DIAM HEPTANE POOL FIRE

Liquid	Flash Point (K)	Fire Point (K)	Auto-Ignition Temp, (K)	Ignition Time (s)
#2 Fuel Oil	397	402	533	150
#6 Residual Oil	419	450	605	120
Mobil DTE-797	480	497	639	255
Pennzoil 30-HD	489	514	650	162
Fyrquel 220	530	586	639	130*

*The fire plume was tilted over the Fyrquel 220 (see plan view, Figure 2-1)

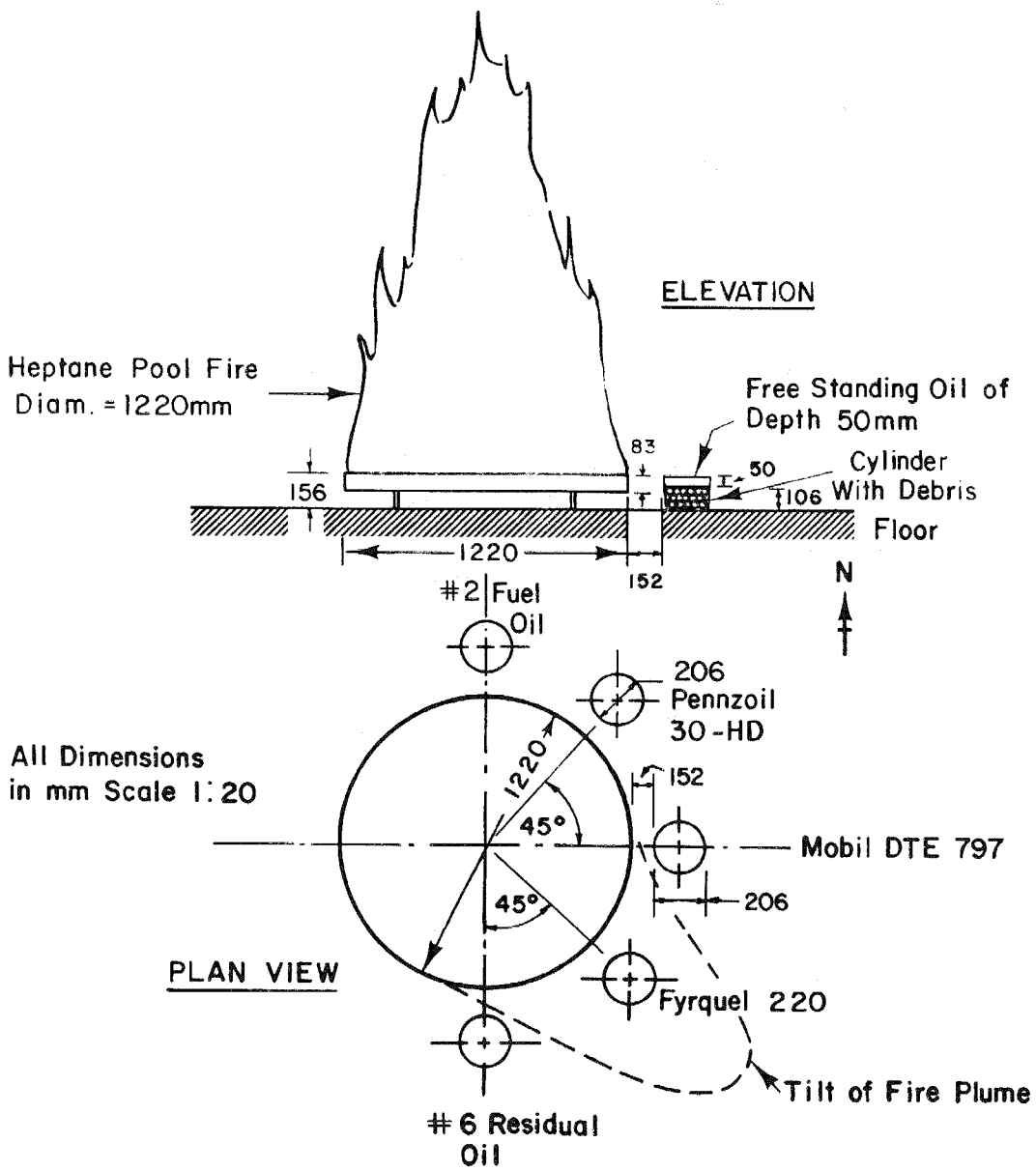

Figure 2-1. Schematic of a large-scale experiment using a heptane source fire of diameter 1.2 m. Cylinders containing the high-fire-point liquids are placed non-contiguous with, but adjacent to the heptane source fire.

The test was conducted in Factory Mutual's 41-m x 82-m x 20-m high enclosed test site which provided a nearly draft-free environment with unrestricted air access.

The heptane pool fire tended to induce asymmetric air currents which generally tilted the fire plume to the southeast as shown by the dotted line in the plan view of Figure 2-1. Theoretical calculations (2,3) indicate that the range of the time-averaged radiation flux to the oil surface from the heptane pool fire was about 20 ± 5 kW/m^2. This range of flux accounts for the asymmetric nature of the fire plume. Because of the flame tilt, the radiation flux to the Fyrquel 220 on the southeast axis probably was at the high end of this range (i.e., 25 kW/m^2); and at the #2 fuel oil at the low end (15 kW/m^2). Table 2-1 shows ignition times of the oils (measured from the time the heptane source fire was ignited). The ignition of the oils was piloted by flamelets from the pulsating heptane fire. All five oils ignited between 120 and 260 s. Table 2-1 appears to show that there is no obvious correlation between fire points and ignition times. The lack of correlation is probably due to the uneven flux distribution caused by the southeasterly tilt of the fire plume. Possibly because of the tilt, the Fyrquel 220 ignited rather quickly* despite its high fire point.

This large-scale test indicates that deep pools of oils spilled on the floor might be expected to ignite in less than 300 s in the presence of an intense fire such as a 1.2-m diam pool fire of heptane.

However, it might be noted that a 1.2-m diam heptane fire is a rather severe fire which by itself represents a serious threat to an electric utility installation regardless of other hazards such as oil spills on the floor of the utility. Determining the additional hazard represented by an oil spill in the vicinity of such an intense fire may be somewhat academic.

2.2 DEEP POOLS OF HYDROCARBON LIQUIDS EXPOSED TO WELD SPATTER OR OXYACETYLENE TORCH

This test simulated ignition of oil by weld spatter falling accidentally into a deep oil spill on the floor of an electric utility. It was assumed that the hot weld spatter falls a vertical distance of 0.5 m through air into the oil spill such as might occur while welding in a kneeling position on the floor adjacent to a spill.

*The Fyrquel 220 fire went out of its own accord soon after the source fire burned out (660 s), whereas the other four oils continued to burn.

A steel rod (cross-section 13 mm x 3 mm thick) was held 0.5 m above the oil containers described in Section 2.1. The rod was melted using an oxyacetylene torch. The molten steel was allowed to fall for 60 s into 50-mm deep layers of oil. Except for the #6 residual oil, none of the oils could be ignited in this manner. The #6 residual oil (which is the most viscous of the five oils tested here) sustained a small flame for about 10 s and then self-extinguished.

An oxyacetylene torch was played for 15 s directly on the surface of each oil. Except for the #6 residual oil, none of the oils ignited by this method, and the flame on the #6 residual oil went out once the torch was removed.

The issue was raised* that deep pools may not represent the most severe test condition because the large volume of oil may rapidly quench the weld spatter. To reduce the quenching effect, the weld spatter tests were repeated with shallow pools of oil, described in Section 2.3.

2.3 SHALLOW POOLS OF HYDROCARBON LIQUIDS EXPOSED TO WELD SPATTER OR OXYACETYLENE TORCH

In this test, the weld spatter was made to fall into 4-mm (shallow) layers of oil on a concrete surface coated with an epoxy protective coating. The concrete and the epoxy coating selected were typical materials (4) used to construct floors in electric utility installations. Because the #6 residual oil is very viscous, it was difficult to form a shallow layer with #6 residual oil; #6 residual oil was not tested in the shallow pool configuration. As before, molten metal was allowed to fall into the oil for 60 s. None of the four oils ignited by this method. An oxyacetylene torch was played for 15 s on the surface of each of the four oils. None of the oils ignited by this method either.

*This issue was raised by Mr. Roy E. Swanson (Project Manager Nuclear Power Division, Electric Power Research Institute) during an interim project review.

Section 3
SMALL-SCALE EXPERIMENTS

Large-scale tests are usually more realistic than small-scale tests but more tedious and expensive and sometimes cannot be conducted in a sufficiently controlled manner. Therefore, it is often desirable to obtain hazard rankings of oil spills based on suitable small-scale tests. A small-scale, hazard ranking apparatus was constructed to classify the hazard presented by oil spills. This apparatus is similar to that constructed previously by Tewarson et al (5). A schematic is shown in Figure 3-1.

3.1 SIMULATION OF RADIANT FLUX FROM A SOURCE FIRE

The flux from a source fire was simulated by four radiant heaters (model 5208, high-density radiant heaters, Research Inc., Minneapolis, Minnesota) mounted on a unistrut frame. Each heater unit consists of six tungsten filament tubular quartz lamps placed in front of an aluminum reflector. The heater body is water cooled and, in addition, the lamp chamber (enclosed behind a 3-mm thick quartz window) is air cooled. Once energized, the lamps reach steady state in a few seconds (90% of output within 3 s). The spectral emission characteristics of the tungsten filaments are, in general, different from that of a blackbody and from that of a source fire of a typical hydrocarbon fuel. For instance, the spectral emissivity of tungsten is (6) ~0.5 in the visible (0.4 to 0.7 μm) region for a broad (300 to 2600 K) temperature range. The total (i.e., averaged over all wavelengths) emissivity of tungsten increases monotonically from 0.032 at 300 K to 0.31 at 2600 K suggesting a sharp drop of spectral emissivity in the infrared. The tubular quartz casing for the tungsten filament and the quartz window in front of the lamp chamber are nearly opaque at wavelengths exceeding ~4 μm. These lamps are meant to simulate the radiant energy (received by an oil spill) from a source fire. Insofar as the spectral characteristics of the lamps differ from that of a real fire, this simulation should be considered to be only an approximation. Later, we shall show that this approximation acquires a special significance when determining the transmission and absorption characteristics of different oils.

The irradiated surface of the oil sample is located 140 mm below the lamps. The choice of distance was dictated by the maximum flux desired (30 kW/m^2) in the

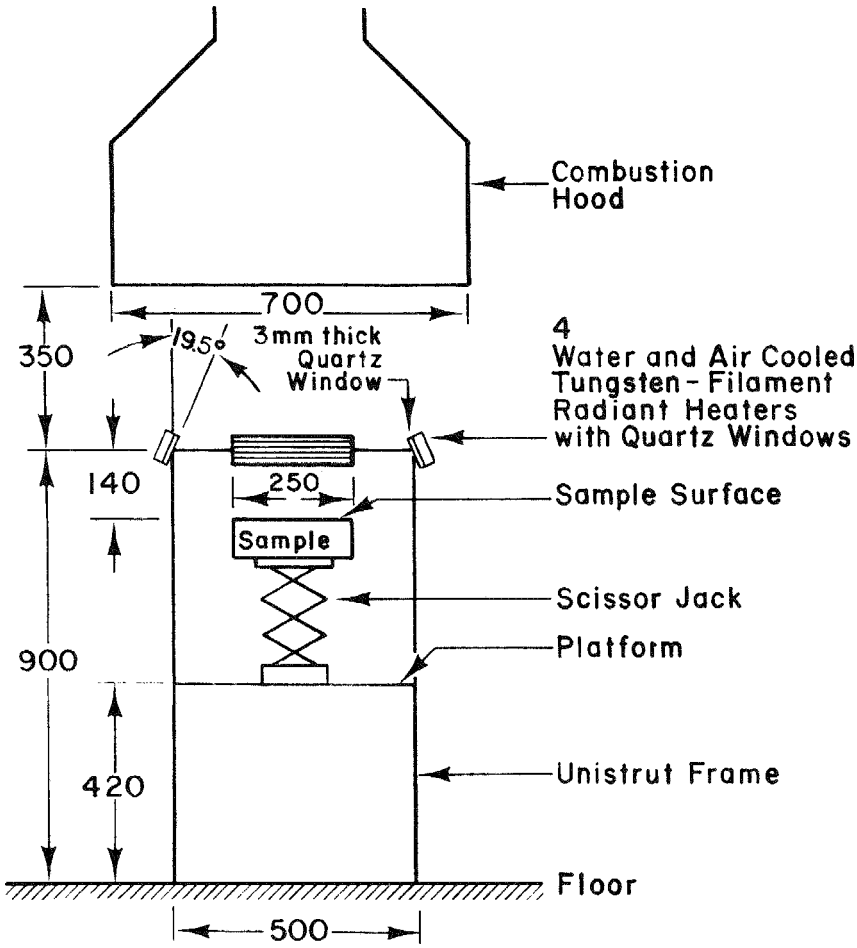

Figure 3-1. Schematic of a small-scale experiment showing radiant heater assembly.

simulation and the maximum safe voltage for driving the lamps. The angle of the lamps was adjusted to produce as even a flux distribution as possible over a sample diameter of 250 mm. Best results were obtained with a 19.5-degree downward tilt (see Figure 3-1) for the lamps. The flux distribution at the sample surface for this configuration is shown in Figure 3-2. The distribution is normalized with respect to the flux at the center. The flux distribution was determined at two voltage settings of the lamps corresponding to a center flux of 21 and 28 kW/m^2 respectively. Figure 3-2 shows that the flux over the sample surface is uniform to within ±7%. The flux is low at the center, peaks at 125 mm diam, then reduces with increasing diameter to ~95% at 250 mm diam. A water-cooled Gardon-type, heat flux gage (Medtherm Corporation, Huntsville, Alabama) was used to measure the flux distribution. Spectral reflectivity effects of the heat flux gage are evident upon comparison of the flux distribution for the two voltage settings of the lamps.

3.2 SIMULATION OF FLOOR MATERIALS IN UTILITY INSTALLATIONS

Floors in a utility installation are made either of concrete or steel. The preponderance of floors are of concrete. Usually the concrete floor is of 21 MPa (3000 psi) strength with a 19-mm maximum aggregate size. A float-finished concrete surface is obtained by smoothing the surface using a two-by-four. The concrete is then cured for about 28 days at atmospheric conditions (294 K; 50% relative humidity). The concrete floor is sometimes coated with two coats of a 0.4-mm (15-mil) thick epoxy finish. If an oil spill occurs in the vicinity of floor-mounted heavy equipment (e.g., a stationary gas turbine), the substrate under the oil spill could be a steel platform supporting the equipment. In the present program three substrate (floor) materials were tested: 1) concrete, 2) epoxy-coated concrete, and 3) steel. The concrete used was Yankee Quikrete (F. B. Jones Manufacturing Co., Inc., Everett, Mass.). The mix consisted of 16% (by weight) Portland cement, 36% concrete sand and 48% pea stone and it tested at approximately 21 MPa pressure. The concrete samples were cast (up to a depth of 55 mm) in 250-mm diam, 70-mm deep aluminum pans and float-finished with a wooden trowel. The concrete was cured for 28 days in a controlled environment chamber at 294 K, 50% relative humidity. After curing, the vertical distance between the concrete surface and the top edge of the aluminum pan was 15 mm. Some roughness was noted on the surface of the cast concrete due to escaping air bubbles during the curing process. Ten such samples were cast and cured in pans.

Four samples were then coated with two coats of Koppers Bitumastic No 300-M protective coating (Koppers Co. Inc., Pittsburgh, Pennsylvania). Bitumatic No 300-M is a coal-tar epoxy chemical, cured protective coating often used (4) to protect concrete floors against corrosive atmosphere and to provide a smooth floor surface.

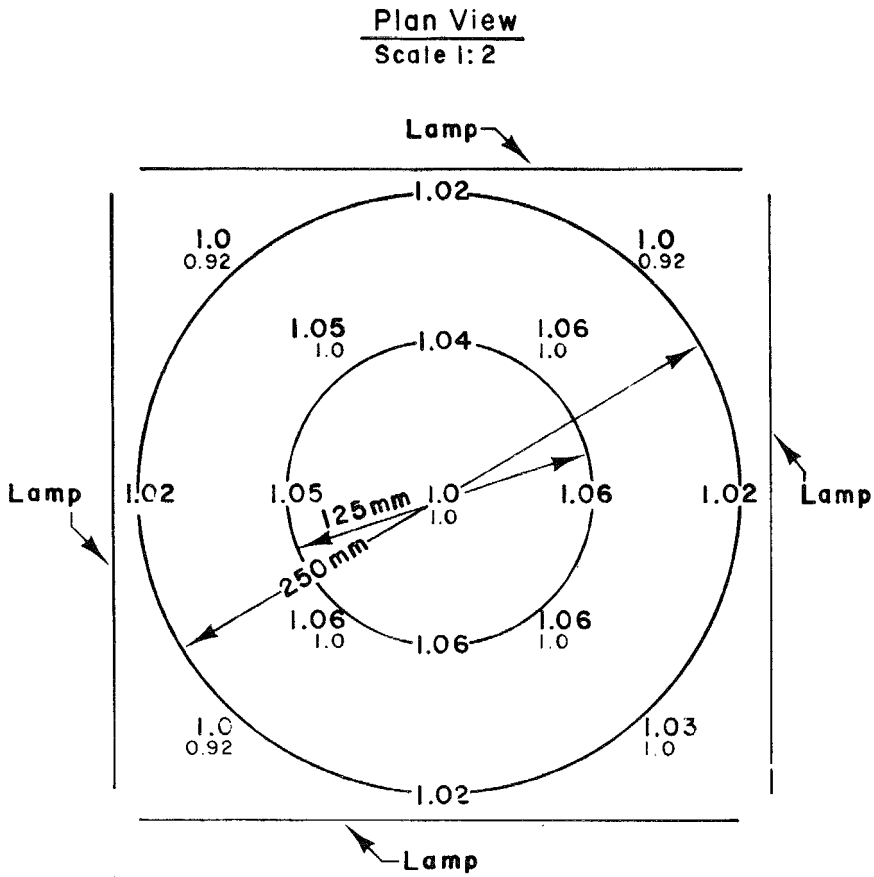

Font	Flux at Center, kW/m^2
Bold	28
Light	21

Figure 3-2. Normalized flux distribution for 2 voltage settings of the tungsten-quartz radiant heater. Bold font indicates 28 kW/m^2 flux at center. Light font indicates 21 kW/m^2 at center. Flux uniformity is within 7 percent for a 250 mm diameter region about the center.

To simulate a steel platform, a 250-mm diam, 25-mm thick AISI C 1018 cold-rolled steel disc was used.

The thermal properties of the epoxy-coated concrete were assumed to be the same as that of uncoated concrete. Steel and concrete thermal properties are shown in Table 3-1. Also shown are the thermal properties of copper (which we will have occasion to use later). The thermal conductivity (λ_2) and volumetric heat capacity ($\rho_2 c_2$) of concrete are functions of temperature. For normal weight concrete made with siliceous aggregate λ_2 decreases from (7,8) 1.9 at 300 K to about 1.7 W/(m•K) at 573 K; $\rho_2 c_2$ increases from 1.8 at 300 K to 2.7 MJ/(m^3•K) at 573 K. In the present work, mean values were used: λ_2 = 1.8 W/(m•K), $\rho_2 c_2$ = 2.1 MJ/(m^3•K).

The thermal conductivity and volumetric heat capacity of steel are weak functions of temperature. Here, they are assumed to be constant.

3.3 THERMAL PROPERTIES OF HYDROCARBON LIQUIDS

The flash and fire points (Cleveland Open Cup Method) and autoignition temperatures of the five oils selected for this study are shown in Table 2-1. Oil specific gravities were measured at room temperature (293 K). From the measured specific gravities, API degrees were computed (for those oils with specific gravities less than unity), using the following relation:

$$\text{API degrees} = \frac{141.5}{G} - 131.5 \qquad 0 < G \leq 1$$

where G is the specific gravity* of oil at 289 K.

Measured specific gravities and their corresponding API degrees are shown in Table 3-2. The thermal conductivity, λ_1; density, ρ_1 and specific heat, c_1, for oils, parametric in API degrees are shown in Figures 3-3 to 3-5 respectively as a function of temperature (11-13). Figure 3-6 shows the volumetric heat capacity $\rho_1 c_1$ for oils as a function of temperature, parametric in API degrees. Figure 3-3 shows that the thermal conductivity varies between 110 and 130 mW/(m•K) in the temperature range of interest (300 to 600 K). A temperature averaged mean value of 125 mW/(m•K) is satisfactory for all five oils in the temperature range 300 to 600 K. Although the density and specific heat vary considerably with temperature, Figure 3-6

*The API scale has been adopted by the American Petroleum Institute for oils with specific gravities less than unity. This scale is not defined for oils (such as Fyrquel 220) whose specific gravity exceeds unity. G was measured at 293 K. It was assumed that G at 289 K was equal to that at 293 K.

Table 3-1

MEAN THERMAL PROPERTIES OF CONCRETE, COPPER AND STEEL

	Thermal Conductivity λ_2, W/(m•K)	Volumetric Heat Capacity $\rho_2 c_2$, MJ/(m^3•K)
Concrete[a] (at 373 K)	1.8	2.10
Copper[b] (at 300 K)	398	3.45
Steel[c] (at 300 K)	46	3.62

[a] Ref (8)

[b] Weast, R.C., Editor, Handbook of Chemistry and Physics, 51st Edition, The Chemical Rubber Co., 1971 p.E-10.

[c] Baumeister and Marks, Standard Handbook for Mechanical Engineers, 7th Edition, McGraw-Hill, New York, N.Y., 1967, p 4-92 Table 1.

Table 3-2

SPECIFIC GRAVITIES AND API DEGREES FOR HYDROCARBON LIQUIDS

Liquid	Specific Gravity at 293 K, G	API Degree
#2 fuel oil	0.88	30
#6 residual oil	0.93	20
Mobil DTE 797	0.86	33
Pennzoil 30-HD	0.95	18
Fyrquel 220	1.13	Not Defined

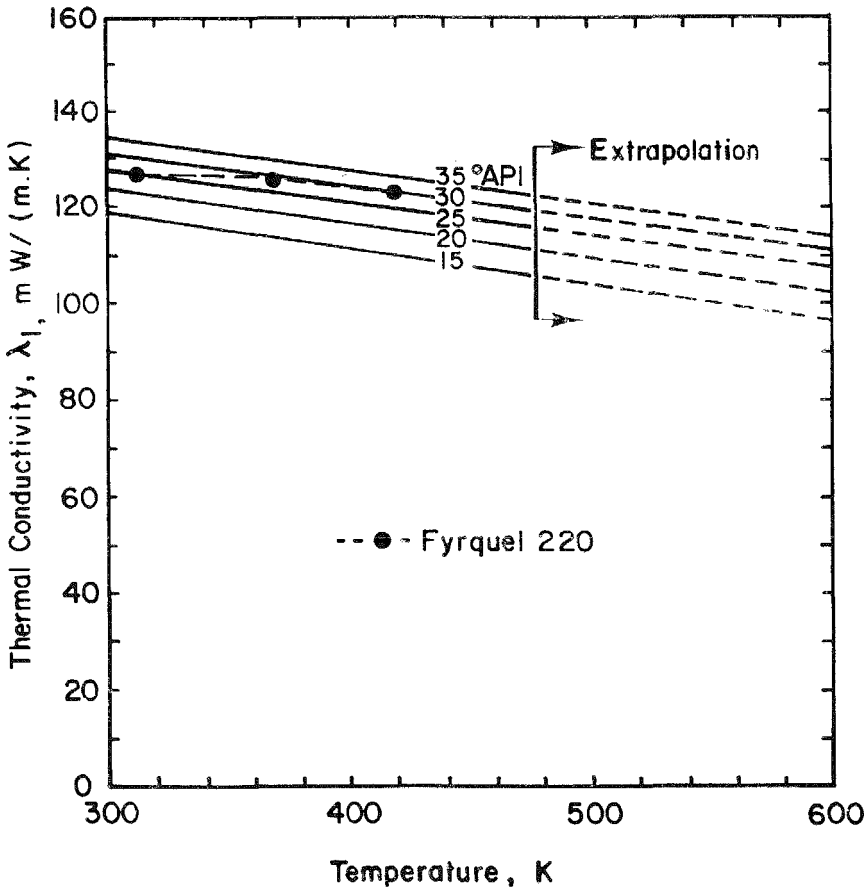

Figure 3-3. Thermal conductivities of hydrocarbon liquids are shown as a function of temperature (300 to 600 K) parametric in API degrees. Thermal conductivity of Fyrquel 220 is shown by the closed circles connected by a dashed line. A temperature averaged mean value of λ-125 mW/(m.K) is reasonable for all hydrocarbon liquids.

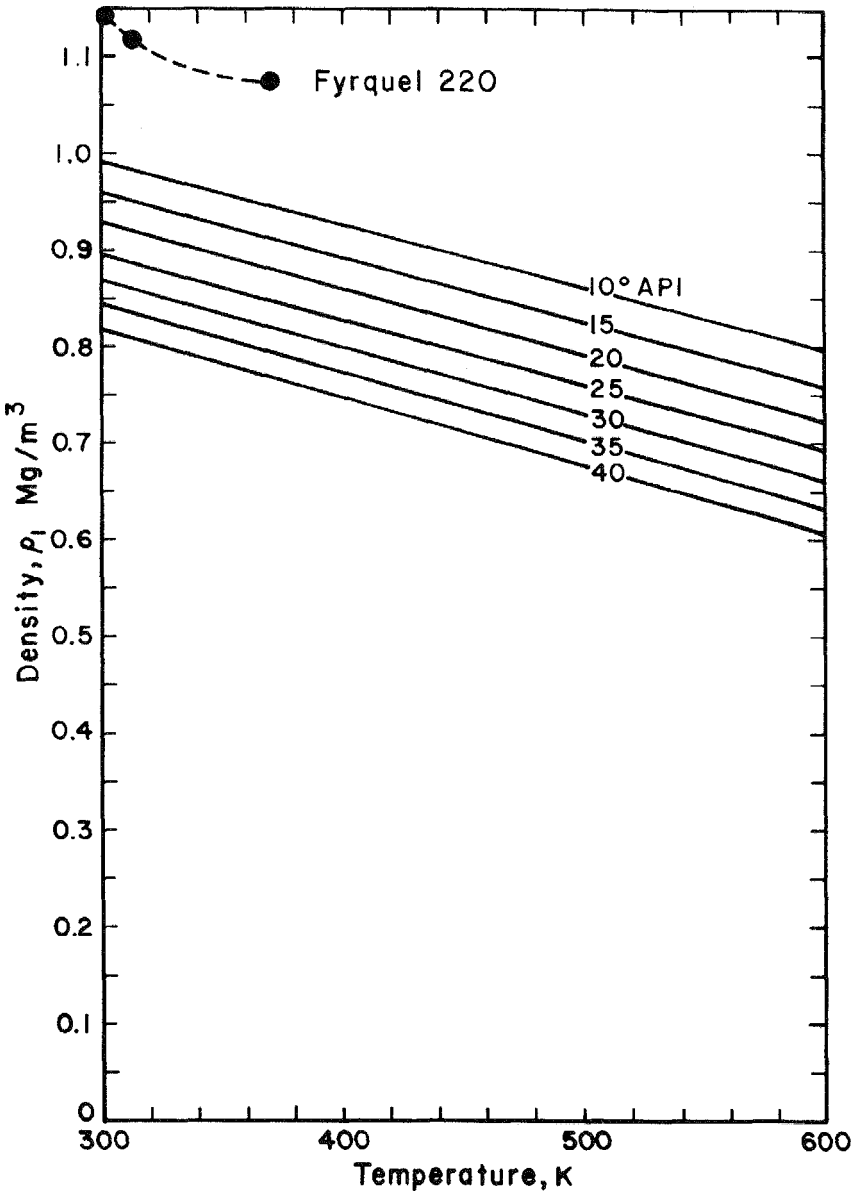

Figure 3-4. Densities of hydrocarbon liquids are shown to decrease with temperature (300 to 600 K). The plot is parametric in API degrees. Density of Fyrquel 220 is shown by the closed circles connected by a dashed line.

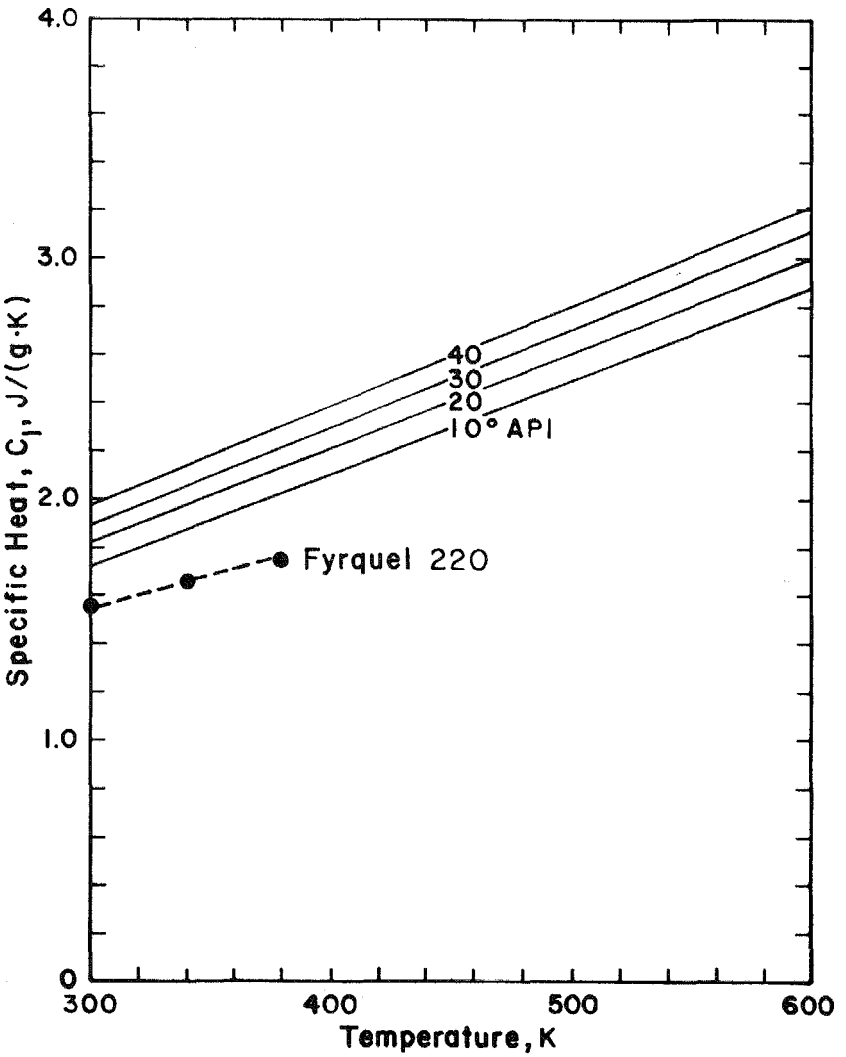

Figure 3-5. Specific heats of hydrocarbon liquids are shown to increase with temperature (300 to 600 K). The plot is parametric in API degrees. Specific heat of Fyrquel 220 is shown by the closed circles connected by a dashed line.

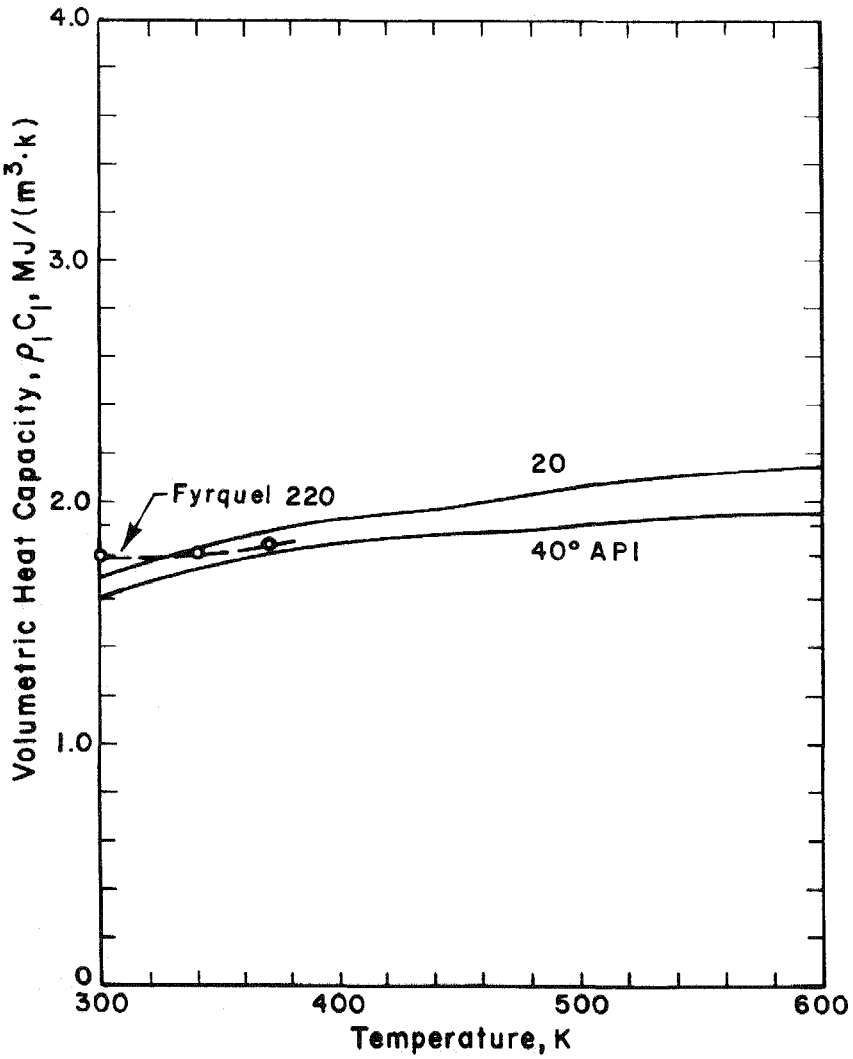

Figure 3-6. Volumetric heat capacities (i.e., product of density and specific heat) of hydrocarbon liquids are shown as a function of temperature (300 to 600 K) parametric in API degrees. Volumetric heat capacity, $\rho_l c_l$, of Fyrquel 220 is shown by the closed circles connected by a dashed line. A temperature averaged mean value $\rho_l c_l$=1.9 MJ/(m^3·K) is reasonable for all hydrocarbon liquids.

shows that the volumetric heat capacity, $\rho_l c_l$, does not. Also, $\rho_l c_l$ appears to be very nearly the same for all oils. A temperature averaged mean value of $\rho_l c_l$ = 1.9 MJ/(m^3•K) appears to be satisfactory for all oils in the temperature range 300 to 600 K.

3.4 INFRARED ABSORPTION AND TRANSMISSION IN HYDROCARBON LIQUIDS

Due to the stretching of the carbon-hydrogen bond, hydrocarbon compounds are active (14,15) in the vicinity of 3.3 μm. As a result, hydrocarbon oils partially absorb and transmit infrared radiation. To demonstrate this effect a glass beaker (85-mm diam; 120-mm deep) filled with Pennzoil 30-HD was exposed to radiant flux (13.8 kW/m^2) from the tungsten-quartz lamps described in Section 2. The sides and bottom of the beaker were insulated with a 5-mm thick ceramic fiber blanket (Cotronics Corporation, Brooklyn, New York). The oil surface was positioned 140 mm below the lamps (see Figure 3-1). Oil surface temperatures were measured with a chromel-alumel (0.13-mm diam wires, bead size 0.13 mm) thermocouple*. Because of thermal expansion, the oil surface rises when exposed to radiation flux. To ensure that the surface temperature was being measured rather than an in-depth temperature, the thermocouple assembly was manually raised (at 30-s intervals) by means of a micrometer screw so that the thermocouple bead maintained a uniform meniscus (noted visually) on the oil surface. The thermocouple wires were made to lie flush with the oil surface. Oil surface temperatures so measured were repeatable to within ±3 K.

The lowest curve in Figure 3-7 shows measured surface temperature rise over ambient (ambient = 299 K) versus time for a 120-mm deep pool of pure Pennzoil 30-HD. Also shown are measured surface temperatures for Pennzoil made progressively less transparent by uniformly mixing the Pennzoil with 5, 10 and 20% by volume of #1 Lampblack 228 83 mixture (Benjamin Moore and Co., Montvale, N. J. 07645), which is a mixture of lampblack ground in linseed oil. As expected, Figure 3-7 shows a surface temperature increase with increasing opacity. The Pennzoil becomes nearly opaque with 10% lampblack addition. Further addition of lampblack mixture does not affect the temperature as shown by the uppermost curve in Figure 3-7 for 10 and 20% addition of lampblack mixture.

Figure 3-7 suggests that the absorption-transmission properties, and therefore, the surface temperature response, of hydrocarbon oils is likely to depend strongly on

---

*In Appendix A we show that the measured surface temperatures do not depend on the diameter of the thermocouple wires or on bead size.

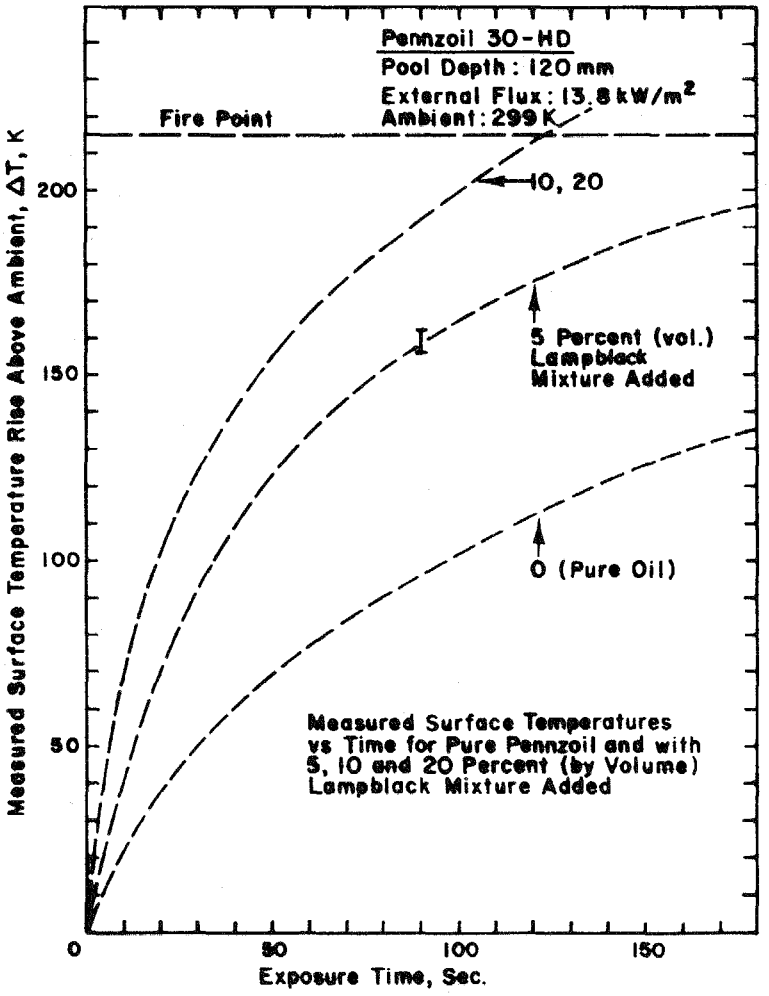

Figure 3-7. Measured surface temperature rise above ambient for a 120 mm deep pool of Pennzoil 30-HD is shown as a function of time of exposure to 13.8 kW/m^2 radiant flux. The 3 measured curves correspond to pure Pennzoil (lowest curve) and Pennzoil made progressively less transparent by addition of #1 Lampblack 228 83 mixture (Benjamin Moore and Co., Montvale, N.J. 07645); lampblack ground in linseed oil). The surface temperature increases with opacity until the oil becomes opaque. Further additions of lampblack does not affect the temperature response. For example, 10 and 20 percent additions of lampblack yield the same response. The vertical bar indicates the test-to-test repeatability of the measurement.

the degree of contamination of the oil. These properties will also depend, to some extent, on the spectral nature of the radiation source. In the present work, it was assumed that the radiation from a hydrocarbon source fire could be approximated by the tungsten-quartz lamps; the degree of validity of this assumption was not tested in the present program.

A quartz beaker (80-mm diam x 60-mm deep x 3-mm thick walls) placed over, but not touching, a Gardon-type heat-flux gage was used to measure the absorption-transmission properties of the oils. The heat flux gage was placed 140 mm below the tungsten-quartz lamps. The lamps were set at 13.8 kW/m^2. The heat flux was measured with and without oil at various depths in the quartz beaker.

In the visible region (5893 Å), the refractive indices of quartz and hydrocarbon oils in air are 1.55 and 1.4, respectively. Kashiwagi (16) has shown that, for these values of the refractive indices, less than 3% of the incident flux is reflected. This reflection was neglected and the transmittance, τ, was computed as a ratio of the fluxes with and without oil in the quartz beaker. Figure 3-8 shows the transmittance plotted as a function of oil depths up to 10 mm for #2 fuel oil, Mobil DTE 797, Pennzoil 30-HD and Fyrquel 220. For comparison, a similar plot for water at room temperature is also shown. In general, water is less transparent than oils. The vertical bar in Figure 3-8 is an indication of the scatter in these measurements. Figure 3-8 shows that all the oils including Fyrquel 220 (a phosphate-ester type oil) possess similar transmission properties. Presumably, this is due to the carbon-hydrogen bond common to all hydrocarbon compounds. The water curve in Figure 3-8 is substantially different from that of the oils.

In Figure 3-8, the straight line tangential to the Pennzoil 30-HD curve may be considered to be a suitable approximation for the transmittance, τ for all oils (except #6 residual oil which is opaque). The equation describing the straight line is given by:

$$\tau = \gamma e^{-kd}$$

where $\gamma = 0.55$ and $k = 48\ m^{-1}$; $(1-\gamma)$ may be considered to be the absorptivity (or emissivity) of the oil surface; k is the spectrally gray absorption-coefficient; d is the oil depth in meters. Similarly, the parameters for water at room temperature are $\gamma = 0.3$ and $k = 44\ m^{-1}$. It should be noted that these values of γ and k strictly apply only for a tungsten-quartz radiation source. However, in the absence of other information, they may be extrapolated to radiation from a source fire in a hydrocarbon fuel.

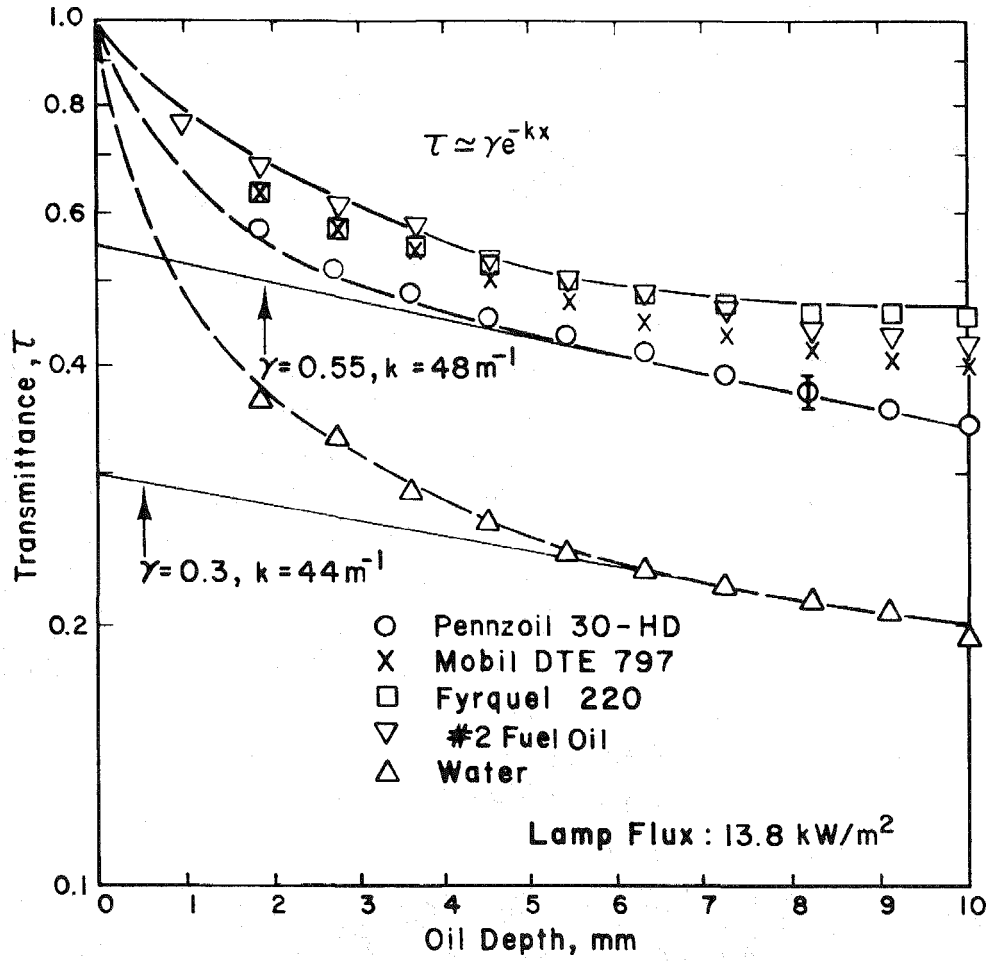

Figure 3-8. Measured transmittance, τ, to thermal radiation from the tungsten-quartz lamps is shown as a function of liquid depths for 4 hydrocarbon liquids and for liquid H_2O. All hydrocarbon liquids show similar transmission properties. Liquid water is less transparent than the oils. The vertical bar shows the scatter in the measurements. The straight line tangential to the Pennzoil 30-HD curve is a satisfactory approximation for all hydrocarbon liquids (except #6 residual oil which is opaque). That straight line is correlated by $\tau = \gamma e^{-kd}$ where $\gamma = 0.55$ and $k = 48\ m^{-1}$. For water, $\gamma = 0.3$ and $k = 44\ m^{-1}$; d is the liquid depth.

Table 3-3 provides a summary of thermal and absorption properties suitable for all hydrocarbon oils in the temperature range 300 to 600 K.

3.5 SURFACE TEMPERATURES FOR DEEP SPILLS OF HYDROCARBON LIQUIDS

Because the thermal as well as absorption-transmission properties of the oils tested are essentially the same, it may be expected that the surface temperature response of all oils will be the same when exposed to an external radiant flux. This is confirmed by experiments as shown in Figures 3-9a and 3-9b. Figure 3-9a shows measured surface temperature response versus time for 120-mm deep pools of #2 fuel oil, Mobil DTE 797, Pennzoil 30-HD and Fyrquel 220. The external flux from the tungsten-quartz lamp was 13.8 kW/m^2. The measured temperatures for all four oils were clustered in the shaded region shown in Figure 3-9a. Figure 3-9b is a similar plot for an external flux of 26 kW/m^2.

The results in Figures 3-9a and 3-9b indicate that the temperature response for deep pools is nearly the same for all hydrocarbon oils.

3.6 DEPTHS OF UNCONFINED SPILLS

In an accidental spill, the volume of flammable liquid spilled can vary considerably: from as low as a few quarts of liquid to as much as hundreds of gallons for accidents in which several drums containing the liquid have ruptured. The time for the liquid to spread depends on the liquid viscosity and the roughness of the floor. Except for the #6 residual oil which is highly viscous, all the liquids studied here spread to a steady state configuration in less than 60 s.

The final depth in an unconfined spill on a truly horizontal floor is independent of the volume spilled. This depth depends on the surface tension of the liquid and the contact angle between the liquid and the substrate. Thus, the depth of spill may be considered to be a property of the liquid-substrate pair.

The depths of unconfined spills on concrete, epoxy-coated concrete, and steel for #2 fuel oil, Mobil DTE 797, Pennzoil 30-HD and Fyrquel 220 were determined by spilling known volumes of oil and measuring the wetted spill areas. An illustrative plot of wetted spill area versus volume is shown in Figure 3-10 for Pennzoil 30-HD. The wetted area versus volume data for both steel as well as epoxy-coated concrete can be correlated by a single line. On uncoated concrete, however, the wetted spill area is less than for coated concrete because of significant oil absorption in the uncoated concrete. Figure 3-10 suggests that, for nonabsorbing substrates the spill depth is primarily a property of the oil and is independent of the substrate

Table 3-3

PROPERTIES OF HYDROCARBON LIQUIDS
(300 - 600 K)

Thermal conductivity λ_l, mW/(m•K)	125
Volumetric heat capacity $\rho_l c_l$, MJ/(m^3•K)	1.9
Surface layer absorption (1-γ)	0.45
Absorption coefficient, k, m^{-1}	48
Fire points, K	400 to 600 K

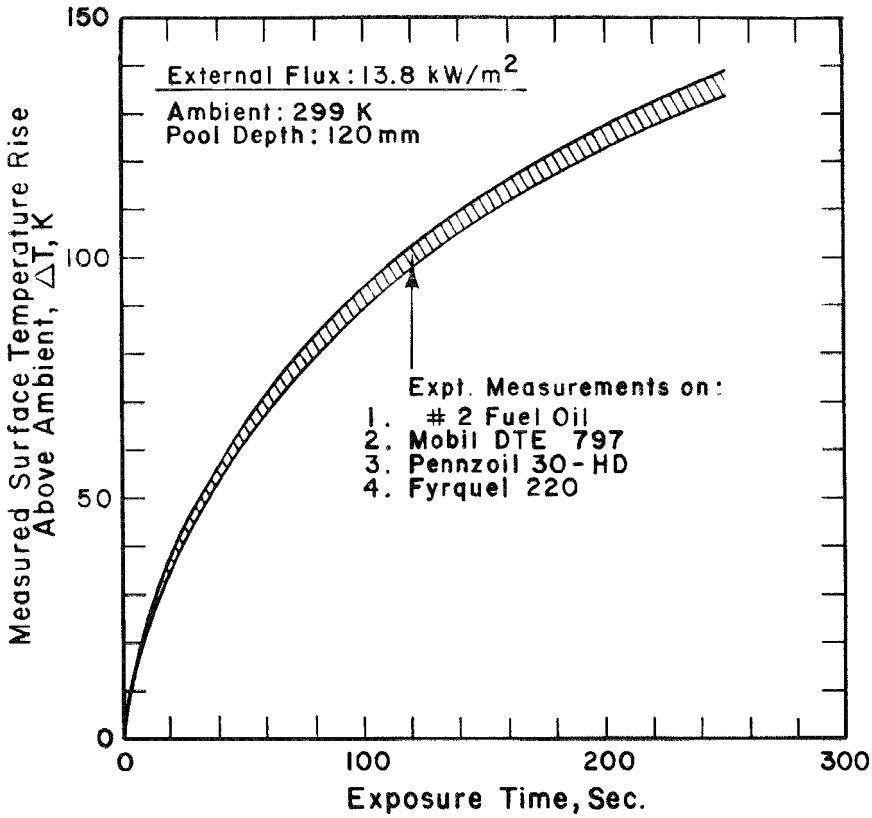

Figure 3-9a. Experimental measurements of surface temperature rise above ambient are shown for 4 hydrocarbon liquids as a function of time of exposure to 13.8 kW/m^2 radiant flux. The hydrocarbon liquid pools were 120 mm deep. The shaded region encompasses the measurements for all four liquids.

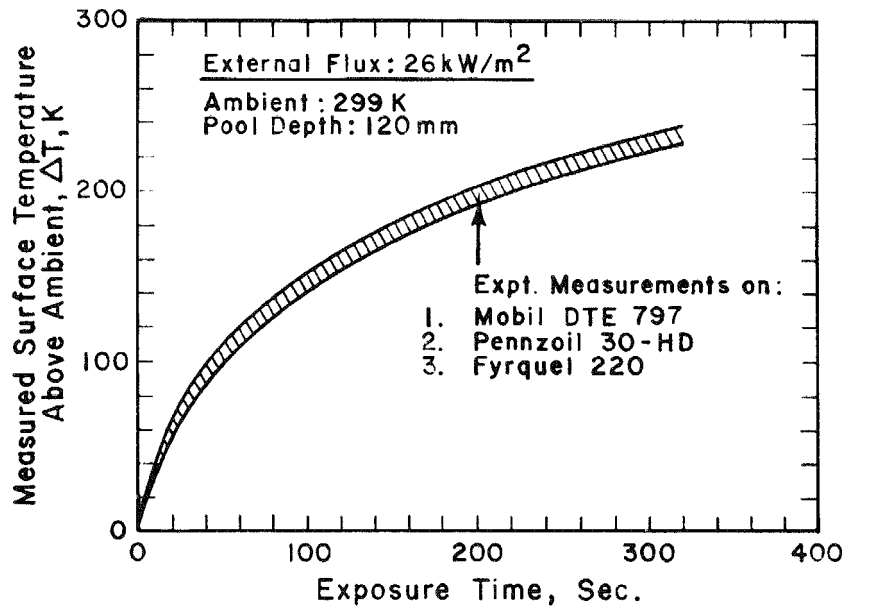

Figure 3-9b. 26 kW/m^2 Radiant Flux.

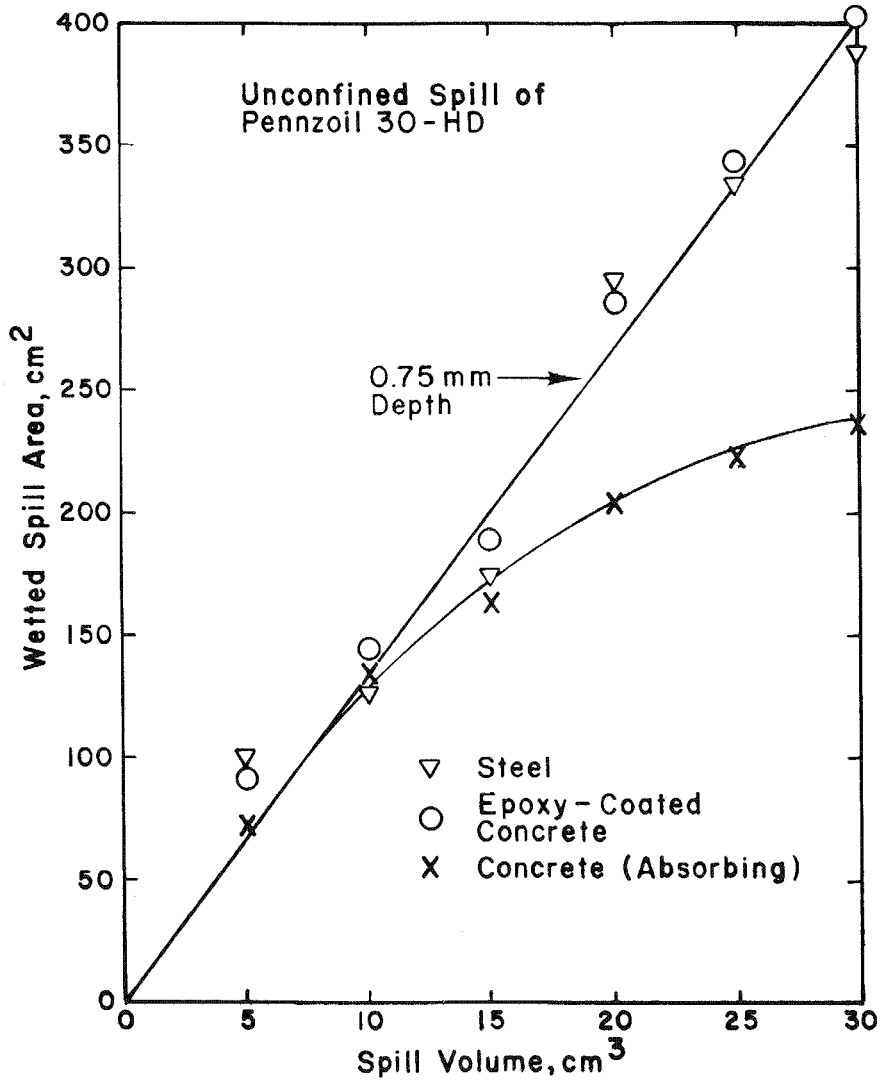

Figure 3-10. Measured spill areas are shown as a function of spill volume for an unconfined spill of Pennzoil 30-HD on three horizontal surfaces: 1) steel 2) epoxy-coated concrete and 3) uncoated concrete. The steel and epoxy-coated concrete data can be correlated by a single striaght line. For uncoated concrete, measured areas are less because of oil absorption into the substrate. The spill depth is given by the reciprocal slope of the straight line. This figure shows that for non-absorbing surfaces, the spill depth is primarily an oil property and it is relatively independent of the surface material.

material. As discussed previously, Figure 3-10 also shows that for nonabsorbing surfaces, the depth of spill is independent of the spill volume. The spill depth for Pennzoil 30-HD on a nonabsorbing substrate is given by the reciprocal slope of the straight line of Figure 3-10. For Pennzoil 30-HD this depth is 0.75 mm. On an absorbing surface (e.g., uncoated concrete), because of absorption into the substrate, the wetted area as well as the spill depth is generally less than that on a nonabsorbing substrate.

Table 3-4 summarizes the results of unconfined spill tests for four oils on nonabsorbing surfaces. In general, an unconfined spill on a nonabsorbing surface is less than a millimeter deep. It may be noted that, although the thermal and transmission properties of oils are similar, unconfined spill depths can vary by as much as a factor of 4 (for the oils tested in this program). Therefore, the surface temperature response of unconfined spills may be expected to vary from oil to oil; the response would also depend upon the thermal properties of the substrate. This result is in contrast to the results obtained for deep pools of oil (Figures 3-9a and 3-9b).

Surface temperatures for unconfined spills on concrete and steel substrates are addressed in Section 3.7.

For a confined spill or a spill on a sloping substrate, the spill depth depends on the liquid volume, the degree of confinement and the tilt angle of the substrate. These factors, in turn, depend on the particular geometry encountered in a given electric utility installation. In general, the liquid depth in a confined spill is expected to be greater than in an unconfined spill. Consequently, the ignition time of a confined spill will depend more on the thermal properties of the liquid than on those of the substrate. Considering this, ignition times for confined spills may be reasonably well approximated by ignition times for thermally thick liquid spills.

3.7 SURFACE TEMPERATURES OF UNCONFINED SPILLS

Oil spills on uncoated concrete generally tend to be absorbed into the substrate and consequently present less of a fire hazard than do spills on nonabsorbing surfaces. Only nonabsorbing substrates were tested in the present program. Unconfined oil spill tests were performed on epoxy-coated concrete and steel.

Figure 3-11a shows the measured surface temperature versus time for unconfined spills on an epoxy-coated concrete surface for four oils of different unconfined spill depths (see Table 3-4). The externally imposed flux on the oil surface was 13.8 kW/m^2. The degree of test-to-test repeatability of these measurements is

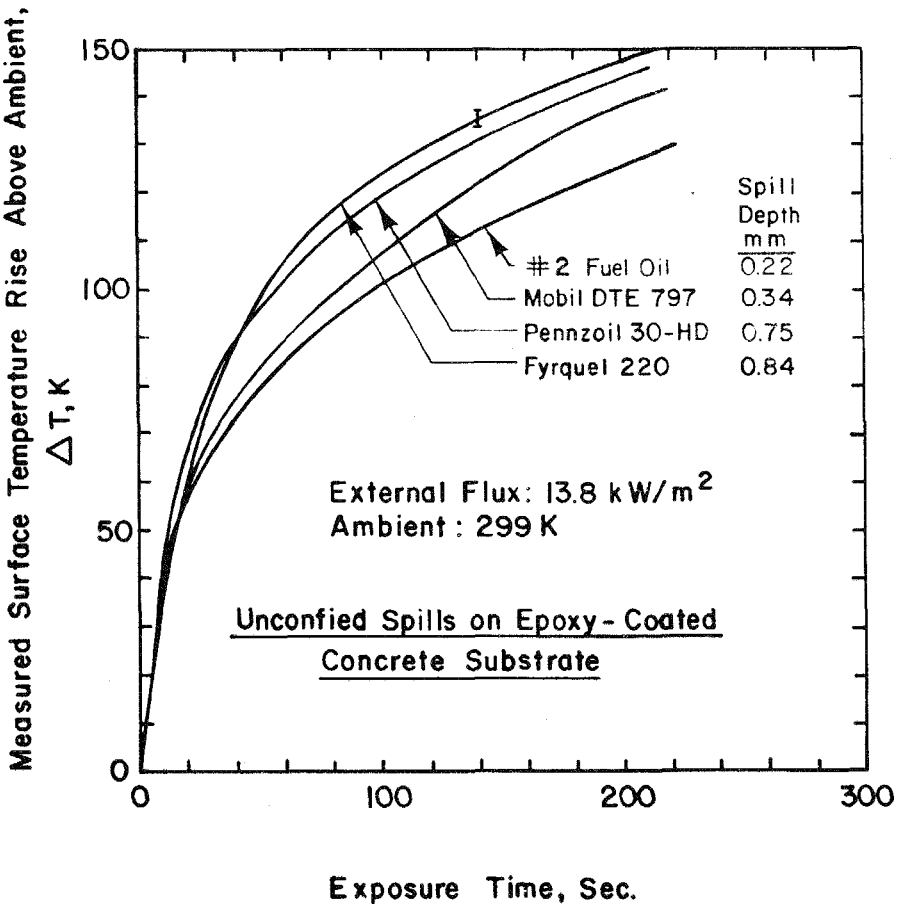

Figure 3-11a. Measured surface temperature rise above ambient is shown as a function of time of exposure to 13.8 kW/m^2 radiant flux, for unconfined spills of four oils on an epoxy-coated concrete substrate. The degree of test-to-test repeatability of the measurements is indicated by the vertical bar. The surface temperature rises faster with increasing spill depth.

Table 3-4

UNCONFINED SPILL DEPTHS FOR HYDROCARBON LIQUIDS
ON EPOXY-COATED CONCRETE AND STEEL

Liquid	Spill Depth (mm)
#2 Fuel oil	0.22
#6 Residual oil	NA
Mobil DTE 797	0.34
Pennzoil 30-HD	0.75
Fyrquel 220	0.84

Table 3-5

COMPARISON OF TIMES TO IGNITION AND FIRE POINT
OIL DEPTH: 120 mm
EXTERNAL FLUX: 26 kW/m^2

Oil	Measured Time to (Piloted) Ignition (s)	Measured Time to Fire Point (s)
#2 fuel oil	30	40
Mobil DTE 797	240	200
Pennzoil 30-HD	210	240
Fyrquel 220	495	500*

*Extrapolated

indicated by the vertical bar in Figure 3-11a.

In general, it can be noted the surface temperature rises faster with increasing spill depth. This trend is attributed to the thermal inertia (i.e., the product of thermal conductivity and volumetric heat capacity, $\lambda\rho c$) of oils being nearly one order of magnitude larger than that of concrete. A similar effect is noted on a steel substrate as shown in Figure 3-11b. The trend reversal between Pennzoil 30-HD and Fyrquel 220 in Figure 3-11b is not significant considering the test-to-test resolution of the temperature data (indicated by the vertical bar).

Comparing Figures 3-11a and 3-11b, it can be seen that the oil surface temperatures on steel are lower than on concrete because steel is a better conductor than concrete. This effect is even more pronounced in Figure 3-12 for an unconfined spill of Fyrquel 220 on epoxy-coated concrete and steel for an externally imposed flux of 26 kW/m^2.

3.8 DEFINITION OF IGNITION TIME

The time to ignition may be defined as the time required to raise the surface temperature of the oil to its (Cleveland Open Cup Method) fire point. The degree of validity of this definition of ignition time is shown in Table 3-5 for 120-mm deep pools of oil exposed to the tungsten-quartz lamps set at 26 kW/m^2. Ignition was achieved by a small pilot flame located 5 mm from the oil surface. Table 3-5 indicates that ignition times correlate reasonably with the time required to raise the oil surface to its fire point. In the present work, the time required to raise the oil surface temperature to its fire point was used as a measure of ignition time.

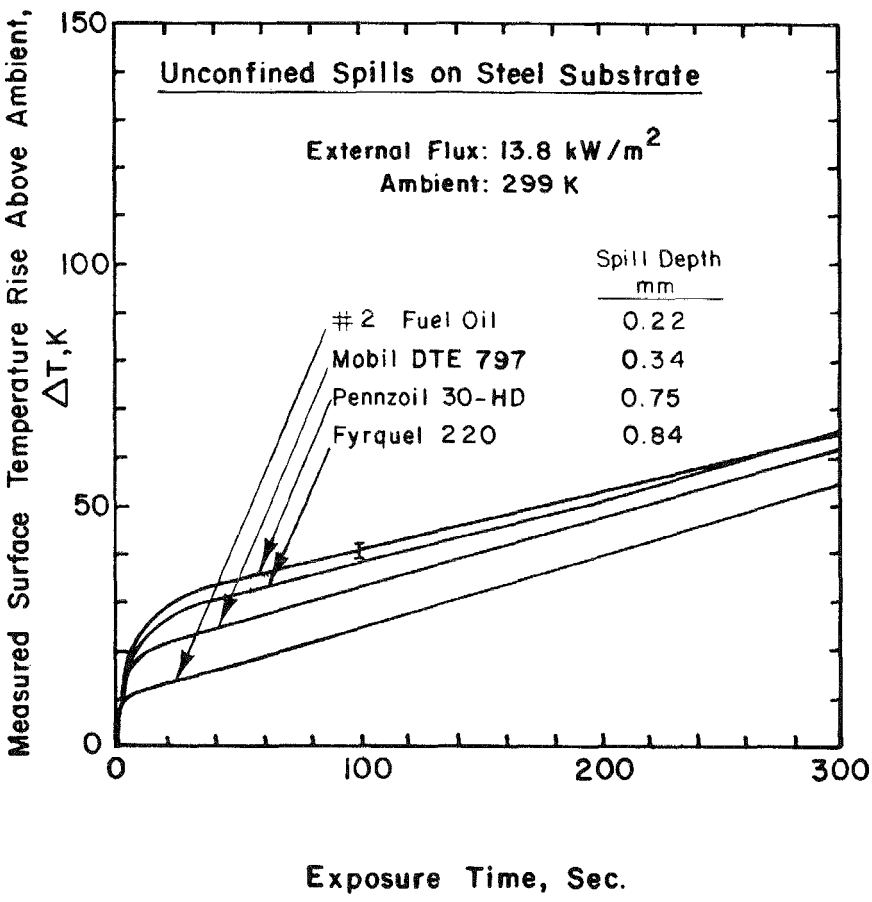

Figure 3-11b. Temperature response of unconfined spills on a steel substrate for four hydrocarbon liquids.

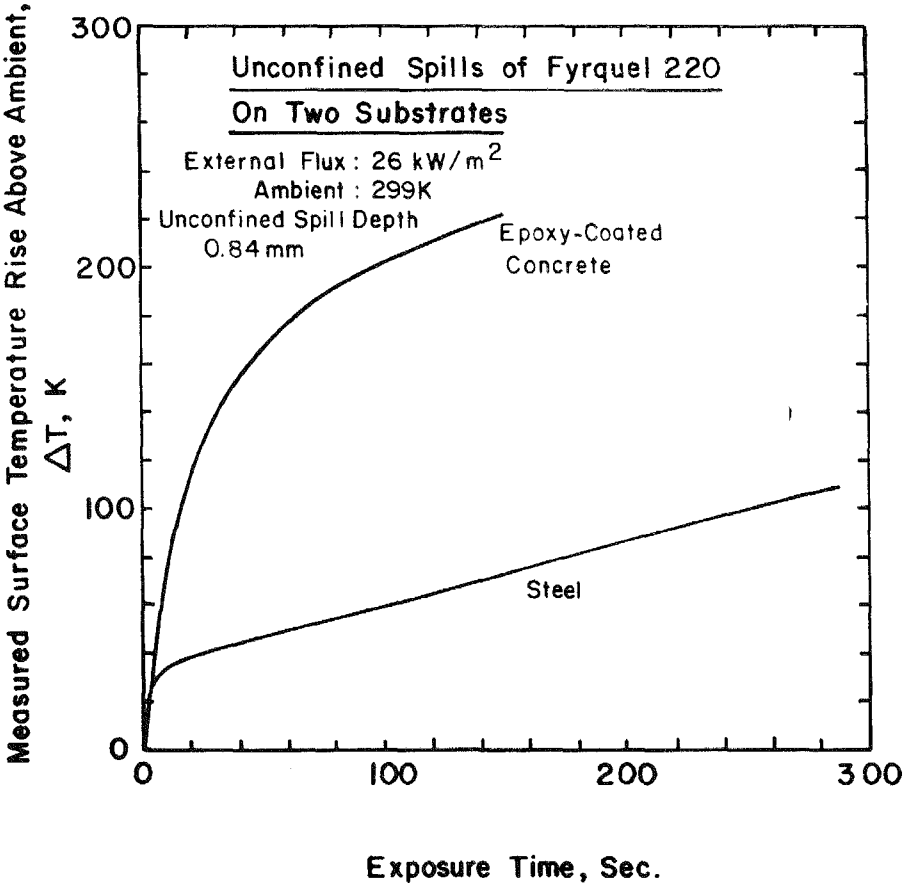

Figure 3-12. Measured surface temperature rise above ambient is shown as a function of time of exposure to 26 kW/m^2 radiant flux for unconfined spills of Fyrquel 220 on 1) epoxy-coated concrete and 2) steel. A strong effect of thermal properties of the substrate on temperature response is evident.

Section 4
THEORY

A simple mathematical model describing the surface temperature response of a semi-transparent oil spill exposed to a thermal radiation flux would have utility. For such a model to be useful, it should be as simple as possible, preferably a closed-form, analytic model. To achieve this, the following simplifying assumptions are necessary:

1. The thermal and absorption-transmission properties of the oil are constant with respect to oil temperature.
2. The substrate under the spill is opaque to thermal radiation.
3. The thermal properties of the substate are constant with respect to temperature.
4. No significant convective heat and mass transfer effects occur within the spill layer.
5. The net flux delivered to the oil surface is constant with time.

In Section 3.3 it was shown that the first assumption is reasonable (see Figures 3-3 and 3-6). The second assumption is generally satisfactory because floors in electric utility installations are usually opaque and nonreflecting. The third assumption is satisfactory to within the accuracy to which concrete or steel composition and properties are known (7,8); it is not an important assumption.

For a uniformly heated oil surface, the fourth assumption is usually quite satisfactory. Excellent reviews by Velarde and Normand (17,18) provide a more detailed understanding of the approximations implicit in assumption 4. The fifth assumption is a strong approximation because, for a constant externally imposed flux, the net flux to the oil surface generally decreases with time due to the following three factors:

1. The oil surface temperature increases with time resulting in increased convective cooling of the oil surface.
2. Because of increasing oil surface temperature, the surface radiation losses increase with time.
3. With increasing surface temperature, the lighter factions of the oil begin to vaporize and form a vapor plume over the oil surface. The vapor density increases with time and the plume absorbs an increasing fraction (16) of the incident radiant flux.

The absorbed fraction also tends to increase with increasing incident flux because of greater vaporization from the oil surface.

Each effect tends to reduce the net flux to the oil surface with time. However, despite these limitations, assumption 5 is still very useful if the surface losses are accounted for in an approximate way. A suitable approximation is discussed in Section 4.1.

4.1 SEMI-INFINITE POOLS OF HYDROCARBON LIQUIDS

Oil spills with depths exceeding 20 mm can be well approximated by a semi-infinite and semi-transparent medium. The temperature-time response of deep spills is independent of the thermal properties of the floor under the spill. This response can be described by a one-dimensional (constant thermal and absorption-transmission property) energy conservation equation given by:

$$\rho_1 c_1 \frac{\partial T_1}{\partial t} = \lambda_1 \frac{\partial^2 T_1}{\partial x^2} + \gamma k \dot{q}'' e^{-kx} \qquad (4\text{-}1)$$

where $\rho_1 c_1$ is the volumetric heat capacity of the oil and λ_1 is its thermal conductivity. The origin (x=0) of the one-dimensional spatial coordinate system is located at the oil surface and x increases with oil depth. $T_1(x,t)$ is the oil temperature at depth x and time t; γ and k are the transmission parameters described in Figure 3-8; $\dot{q}''$ is the (constant) net flux to the oil surface. The boundary conditions are:

$$-\lambda_1 \frac{\partial T_1}{\partial x}\bigg|_{x=0} = \dot{q}'' \qquad (4\text{-}2a)$$

and

$$T_1(\infty,t) = T_0 \qquad (4\text{-}2b)$$

The initial condition is:

$$T_1(x,0) = T_0 \qquad (4\text{-}3)$$

where T_0 is the ambient temperature. A closed-form, analytic solution for $T_1(x,t)$ of Eq. 4-1 with its associated boundary (Eqs. 4-2a and 4-2b) and initial conditions (Eq. 4-3) is obtained by using Laplace transforms (see Refs 3 and 19). The solution for the surface temperature, $T_1(0,t)$, is given by (3):

$$\frac{[T_1(0,t) - T_0]}{\dot{q}''} = 2\left(\frac{t}{\pi\lambda_1\rho_1 c_1}\right)^{1/2} - \frac{\gamma}{k\lambda_1}\left\{1 - e^{-k^2\alpha_1 t}\,\mathrm{erfc}\,(k\sqrt{\alpha_1 t})\right\} \qquad (4\text{-}4)$$

where $\alpha_1 = \lambda_1/\rho_1 c_1$ is the thermal diffusivity of the oil. The first term in Eq. 4-4 represents the classical (20) solution for a non-transparent ($\gamma = 0$ or $k \to \infty$) medium:

$$\Delta T = 2\dot{q}''\left(\frac{t}{\pi\lambda_1\rho_1 c_1}\right)^{1/2} \qquad (4\text{-}5)$$

where $\Delta T = [T_1(0,t) - T_0]$ is the surface temperature rise above ambient.

4.1.1 Comparison of Equation 4-5 with Experiments

An example of an opaque, semi-infinite medium is a deep (120-mm) pool of Pennzoil 30-HD made opaque by adding 10% by volume of #1 Lampblack 228 83 mixture (see uppermost curve in Figure 3-7). To test assumption 5, Eq. 4-5 was compared in Figure 4-1 with measured surface temperatures of the Pennzoil-lampblack mixture. The measured curve in Figure 4-1 is the same as the upper curve in Figure 3-7. The data scatter (i.e., test-to-test repeatability) is indicated by the vertical bar.

The three theoretical curves in Figure 4-1 assume that the net flux $\dot{q}''$ in Eq. 4-5 equals 13.8, 8.9 and 6.8 kW/m^2 respectively. The upper theoretical curve ($\dot{q}'' = 13.8$ kW/m^2) corresponds to a net flux to the oil surface assuming no losses. The lowest theoretical curve assumes that the surface loses 3 kW/m^2 by convection (based on a convective heat transfer coefficient (21,22) h = 13 W/m^2•K) and 4 kW/m^2 by surface radiation (based on unity surface emissivity and a fire point surface temperature, 514 K). The middle theoretical curve assumes a (constant mean convection loss of 1.5 kW/m^2, (constant) mean surface radiation loss of 2 kW/m^2 and an incident flux attenuation of 10% (13.8 x 0.1 = 1.4 kW/m^2) to yield a net flux*, $\dot{q}''$ (13.8 - 1.5 - 2 - 1.4) = 8.9 kW/m^2. The 10% vapor attenuation effect was estimated on the basis of measurements made with a Medtherm heat flux gage located under a quartz beaker containing a vaporizing mixture of Pennzoil and lampblack, exposed to an external flux of 13.8 kW/m^2.

*A net flux of 8.9 kW/m^2 is 65% of the total incident flux of 13.8 kW/m^2.

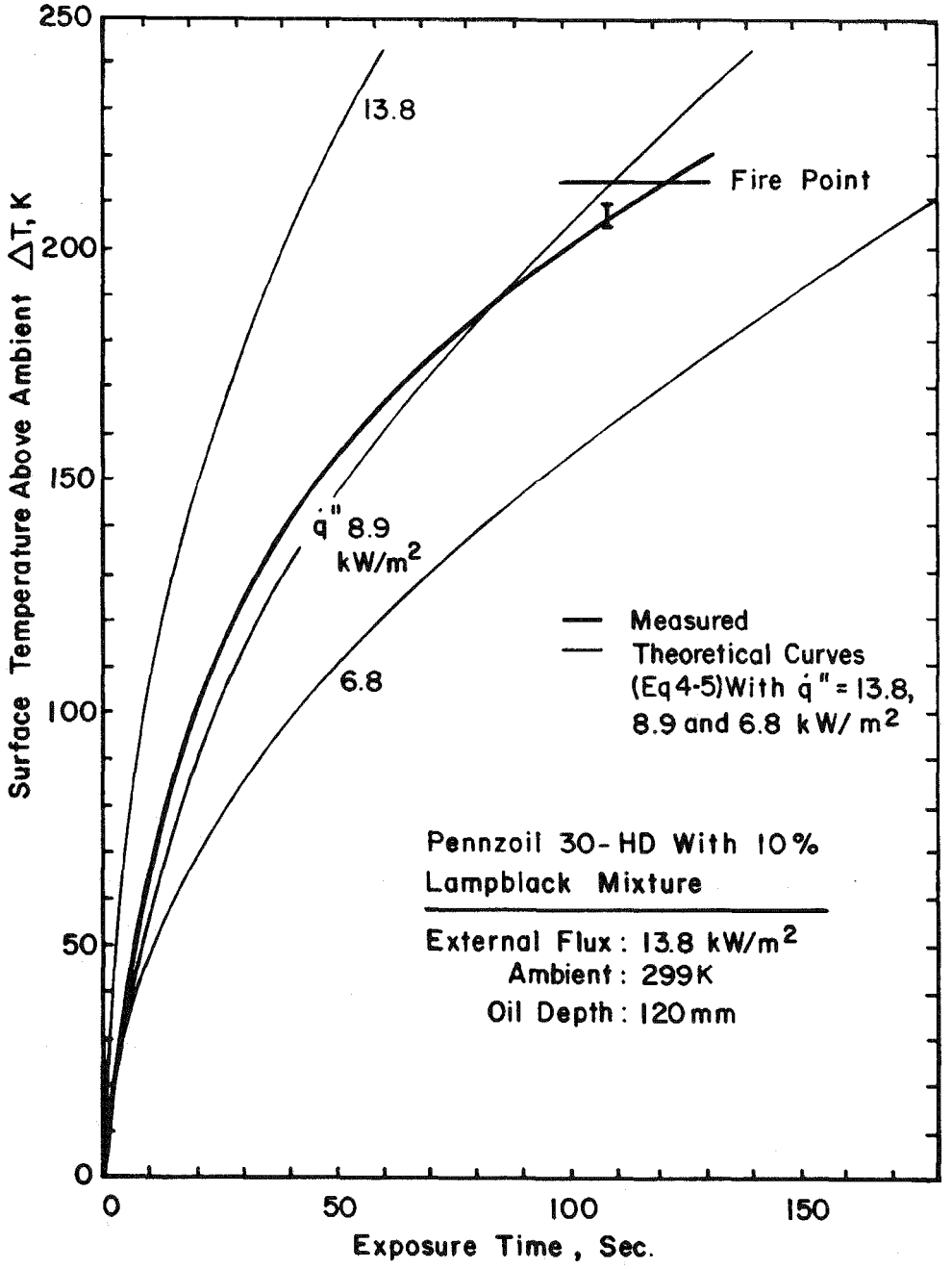

Figure 4-1. Measured surface temperature of an opaque (Pennzoil 30-HD with 10 percent by volume lampblack mixture added), semi-infinite (120 mm deep), medium is compared with theory (eq 4-5) using three different values of net flux $\dot{q}''$=13.8, 8.9 and 6.8 kW/m^2. For an external flux of 13.8 kW/m^2, the measured temperature is best correlated by a net flux $\dot{q}''$=8.9 kW/m^2. The net flux is lower than the external flux because of convection and surface radiation loses and absorption in the vapor plume above the oil surface.

The middle theoretical curve tends to underestimate the early time response of the surface temperature presumably because the losses are overestimated in that time period. At later times, the temperature is somewhat overestimated. This is an inherent limitation of a constant flux model. The model predicts that the time to ignition (i.e., the time to reach fire point) for this system is 110 s, whereas experimental measurements show that the time is about 125 s.

Figure 3-7 emphasizes the fact that surface losses and vapor absorption effects play an important role in reducing the net incident flux and thereby affecting the surface temperature response of the oil spill.

4.1.2 Comparison of Equation 4-4 with Experiments

Figure 4-2a shows a comparison of Eq. 4-4 with measured temperatures for semi-transparent oils with $\gamma = 0.55$, $k = 48\ m^{-1}$. For the experimental measurements, the tungsten-quartz lamps were set at 13.8 kW/m^2. The surface emissivity of semi-transparent oils was approximated by $1 - \gamma = 0.45$. The mean surface radiation loss was estimated using a surface emissivity of 0.45 ($0.45 \times \sigma T^4/2 = 0.9\ kW/m^2$; where $T = 514$ K). The net flux* $\dot{q}''$ used in Eq. 4-4 was ($13.8 - 1.5 - 0.9 - 1.4 =$) 10 kW/m^2. In Figure 4-2a the shaded region representing the experimental measurements is the same as that shown in Figure 3-9a.

Figure 4-2b shows a similar comparison of measurements (the same as the measurements shown in Figure 3-9b) and theory for an external flux of 26 kW/m^2. In this case the temperature data appear to be best correlated using a net flux** $\dot{q}'' = 15.6\ kW/m^2$ in Eq. 4-4. This value is somewhat low. There could be two possible reasons for such a low value. First, the spectral transparency of the oils could well be greater than that shown in Figure 3-8 where the lamps were set at 13.8 kW/m^2 (i.e., γ could be greater than 0.55). Second, the vapor absorption effect could be greater than 10% because of the greater vapor density brought about by the increased flux from the lamps. We believe that the first effect is the larger of the two.

*A net flux of 10 kW/m^2 represents 72% of the total incident flux of 13.8 kW/m^2.
**A net flux of 15.6 kW/m^2 represents 60% of the total incident flux of 26 kW/m^2. Based on net fluxes estimated in Sections 4.1.1 and 4.1.2 it is reasonable to assume that about 65% of the total incident flux is delivered as net flux to the liquid surface.

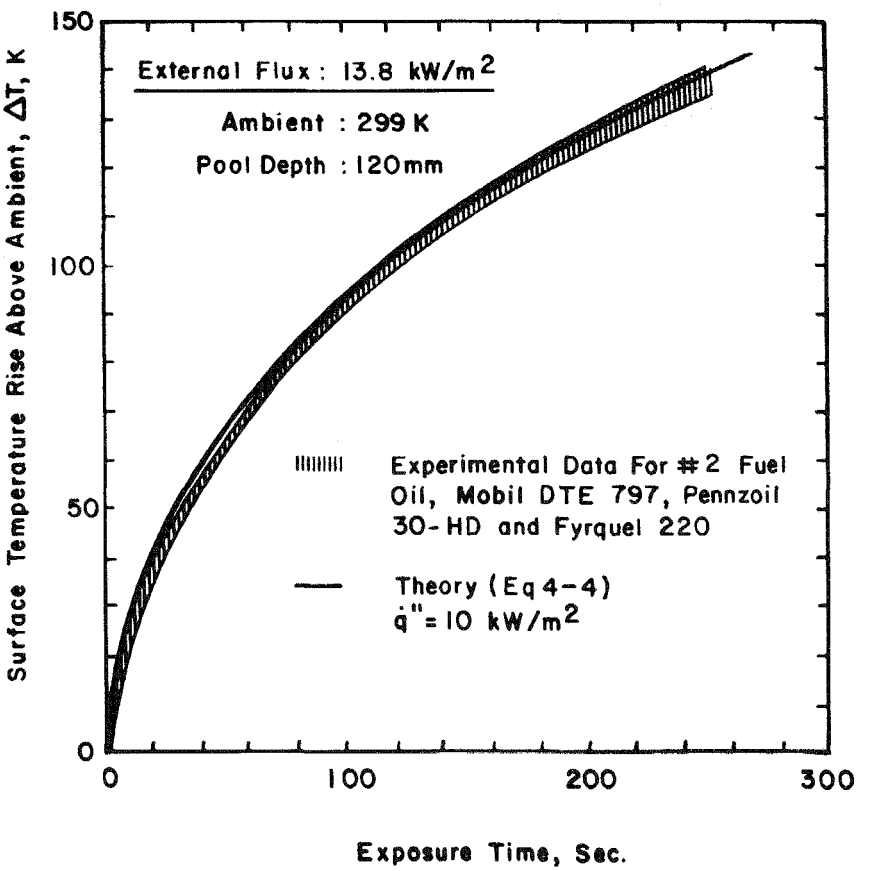

Figure 4-2a. Measured surface temperatures (shaded region) of four semi-transparent, semi-infinite, hydrocarbon liquids are compared with theory (eq 4-4) using a net flux $\dot{q}"$=10 kW/m^2 for an external flux of 13.8 kW/m^2 from the tungsten-quartz lamps.

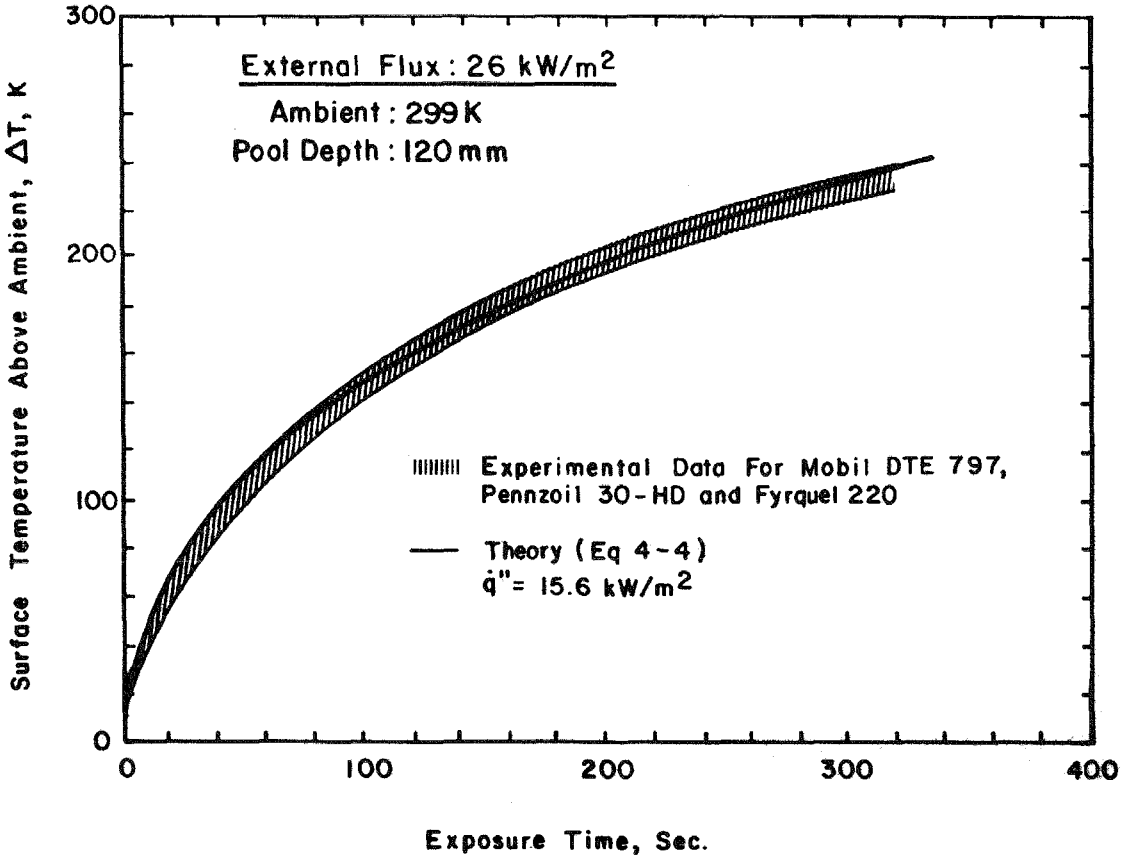

Figure 4-2b. Comparison of theory (solid line) and experiment (shaded region) for 26 kW/m^2 external flux.

4.2 SPILLS OF FINITE DEPTH

Although it is difficult to obtain a general closed-form analytic solution for spills which are of finite depth and are also semi-transparent, simple solution are possible for two important limiting cases. The two limiting cases are finite depth spills of oils 1) opaque to the incident thermal radiation and 2) fully transparent to thermal radiation. In the first case, radiant energy is deposited at the top surface of the spill and in the second case, at the spill-substrate interface. Those two limiting solutions are useful because they may be able to bracket the surface temperature response of a spill which is semi-transparent (i.e., neither opaque nor fully transparent but somewhere in between) to thermal radiation. The two limiting solutions are expected to be especially useful for thin spills because the thinner the spill, the closer the two solutions are to each other. Since the depths of unconfined spills are indeed thin (less than 1 mm; see Table 3-4), the two limiting solutions may be adequate for our purpose. The degree to which those limiting solutions bracket the experimentally measured temperature response is shown in Section 4.2.3.

4.2.1 Finite Depth Spills Opaque to Thermal Radiation

Consider a layer of finite depth, d, of flammable liquid, opaque to thermal radiation, spilled over a (thermally thick) substrate. Assume that the liquid surface receives a constant net flux, $\dot{q}''$, for time $t>0$. A schematic of this one-dimensional system is shown in Figure 4-3. It is assumed that the liquid and substrate are in intimate thermal contact at the interface (i.e., there is no contact resistance at the interface). The energy equation for the liquid layer* is:

$$\frac{\partial T_1}{\partial t} = \alpha_1 \frac{\partial^2 T_1}{\partial x^2} \qquad 0 \leq x \leq d \quad ; \tag{4-6}$$

where T_1 (x,t) is the temperature of the (opaque) liquid at depth, x, and time, t; $\alpha_1 = \lambda_1/\rho_1 c_1$ is the thermal diffusivity of the liquid. The equation for the semi-infinite substrate is:

$$\frac{\partial T_2}{\partial t} = \alpha_2 \frac{\partial^2 T_2}{\partial x^2} \qquad d \leq x \leq \infty \quad . \tag{4-7}$$

*Subscripts 1 and 2 refer to the liquid and substrate, respectively.

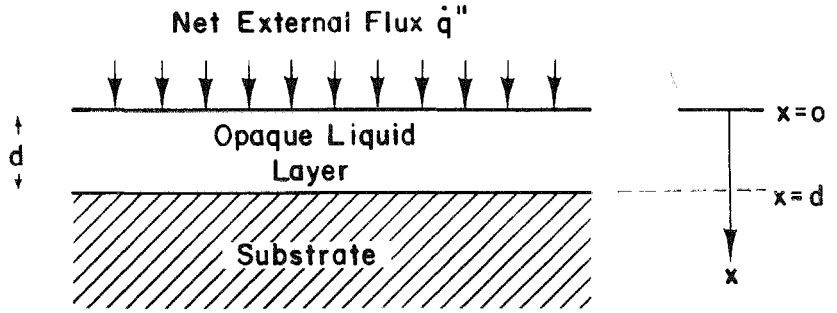

Schematic Of An Opaque, Finite Depth Spill on a Substrate

Figure 4-3. Schematic of a one-dimensional system showing an opaque, finite depth spill on a semi-infinite substrate. The origin (x=0) of the one-dimensional coordinate system is located at the top surface of the liquid spill of depth d. The liquid-substrate interface is located at x=d. For an opaque spill, the net flux, $\dot{q}''$, is delivered at the top surface of the liquid spill. For a fully transparent spill (not shown) the radiant flux is delivered at the liquid-surface interface.

where $T_2(x,t)$ is the temperature of the substrate at depth x and time t; $\alpha_2 = \lambda_2/\rho_2 c_2$ is the thermal diffusivity of the substrate. The interface boundary conditions are:

$$\lambda_1 \frac{\partial T_1}{\partial x}\bigg|_{x=d} = \lambda_2 \frac{\partial T_2}{\partial x}\bigg|_{x=d} \quad , \tag{4-8}$$

and

$$T_1\ (x=d) = T_2\ (x=d) \tag{4-9}$$

The initial condition is:

$$T_1 = T_2 = T_0 \text{ at } t = 0 \tag{4-10}$$

where T_0 is the initial (ambient) temperature of the system. The boundary condition at the liquid surface is:

$$-\lambda_1 \frac{\partial T_1}{\partial x}\bigg|_{x=0} = \dot{q}'' \quad . \tag{4-11}$$

The solution to the two simultaneous partial differential equations, 4-6 and 4-7 with the associated boundary and initial conditions (Eqs. 4-8 to 4-10) may be solved by the method of Laplace transforms (see Appendix B). The solution, $T_1\ (x,t)$, for the liquid layer is given by:

$$T_1\ (x,t) - T_0 = 2\dot{q}'' \left(\frac{t}{\lambda_1 \rho_1 c_1}\right)^{1/2} \left\{ \text{ierfc}\left(\frac{x}{2\sqrt{\alpha_1 t}}\right) + \sum_{n=1}^{\infty} \sigma^n \left[\text{ierfc}\left(\frac{2nd+x}{2\sqrt{\alpha_1 t}}\right) + \text{ierfc}\left(\frac{2nd-x}{2\sqrt{\alpha_1 t}}\right) \right] \right\} \quad ; \text{ for } 0 \leq x \leq d \quad . \tag{4-12}$$

Here, σ is the ratio (1-m)/(1+m) where m is defined by

$$m = (\lambda_2 \rho_2 c_2 / \lambda_1 \rho_1 c_1)^{1/2} \quad ; \tag{4-13}$$

and ierfc (x) is the integral of the error function:

$$\text{ierfc}(x) = \frac{e^{-x^2}}{\sqrt{\pi}} - x\ \text{erfc}\ (x) \tag{4-14}$$

The parameter σ in Eq. 4-12 lies between -1 (σ = -1 implies a highly conducting substrate) and 1 (insulating substrate).

The time-dependent temperature rise over ambient, ΔT, of the liquid surface is obtained by putting x=0 in Eq. 4-12:

$$\Delta T = 2\dot{q}'' \left(\frac{t}{\pi\lambda_1\rho_1 c_1}\right)^{1/2} \left[1 + 2\sqrt{\pi} \sum_{n=1}^{\infty} \sigma^n \, \text{ierfc}\left(\frac{nd}{\sqrt{\alpha_1 t}}\right)\right] ; \qquad (4\text{-}15)$$

Equation 4-15 shows some familiar features: for large values of the parameter $\left(\frac{d}{\sqrt{\alpha_1 t}}\right)$, Eq. 4-15 yields the familiar solution for an opaque semi-infinite spill. For (thin spills) $\frac{d}{\sqrt{\alpha_1 t}} \to 0$, Eq. 4-15 reduces to:

$$\Delta T = 2\dot{q}'' \left(\frac{t}{\pi\lambda_2\rho_2 c_2}\right)^{1/2} . \qquad (4\text{-}16)$$

Equation 4-16 implies that the temperature response of the thin spill is essentially the same as the surface temperature response of the semi-infinite substrate over which the (thin) layer of oil is spilled.

Comparison of Equation 4-15 with Experiments

To verify the accuracy of the finite depth model, a copper-constantan thermocouple was soldered* to the surface of a copper cylinder (99.9% purity; diam 103 mm; height 103 mm). The top surface of the copper cylinder was spray painted with a light coat of spectrally flat black paint. The sides and base of the copper cylinder were insulated with a 5-mm thick ceramic fiber blanket (Cotronics Corporation, Brooklyn, New York). The top surface of the copper was placed 140 mm below the lamps which were set to deliver 20.2 kW/m^2 to the center of the copper surface. The experimental measurements are shown by the heavy line in Figure 4-4. The vertical bar indicates the test-to-test repeatability of the temperature data. The light line represents Eq. 4-15 using thermal properties for pure copper (see Table 3-1). Since the copper cylinder was insulated at the rear surface, the parameter σ=1 in Eq. 4-15. For comparison, a theoretical curve for a semi-infinite copper cylinder is also shown (dashed line). Since copper is a good conductor, for a 103-mm thick copper cylinder finite depth effects are important.

*For accurate surface temperature measurements, intimate thermal contact between the thermocouple bead and the surface is essential.

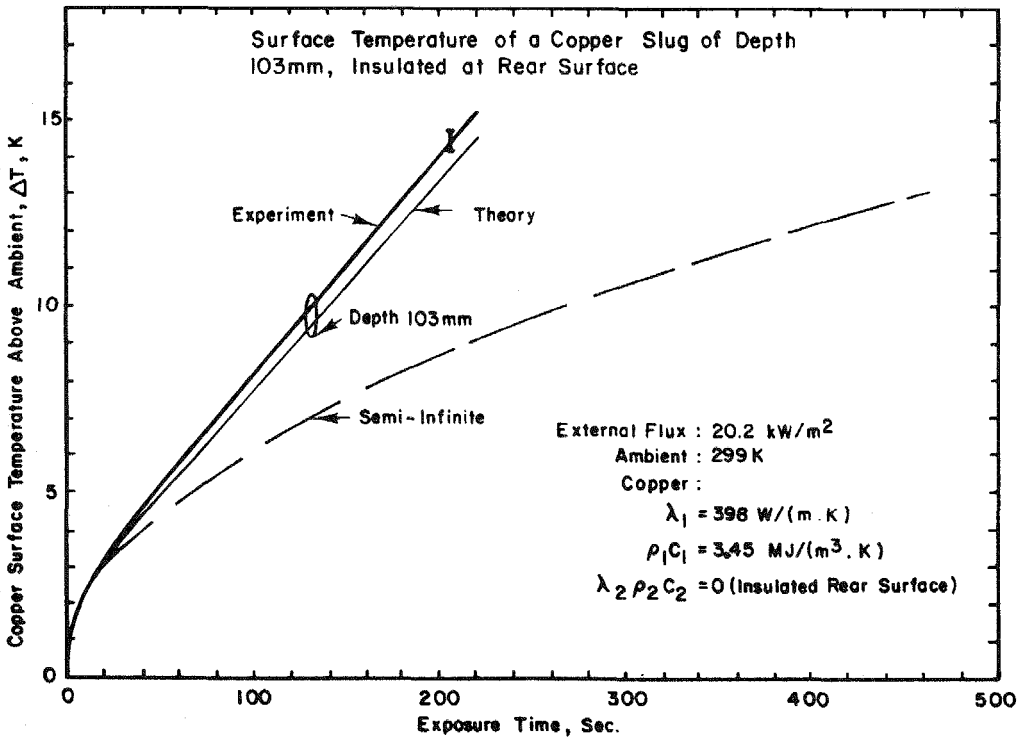

Figure 4-4. Measured (heavy line) surface temperature of a (99.9 percent purity) copper cylinder of finite depth (103 mm) is compared with the finite depth theory of eq (4-15) using $\dot{q}''$=20.2 kW/m^2. The test-to-test repeatability of the measurements is shown by the vertical bar. The external flux from the lamps was 20.2 kW/m^2. The theory slightly underpredicts the measurements because the mean flux was slightly greater than the center flux of 20.2 kW/m^2. This was due to the uneven flux distribution shown in Figure 3-2. The dashed line shows a theoretical curve for a semi-infinite copper cylinder (eq 4-5). It is apparent that, for a 103 mm deep copper cylinder, finite depth effects are quite important.

The theoretical curve (for 103-mm depth) shown in Figure 4-4 underestimates the temperature rise by about 5%. This is primarily due to the slight nonuniformity in the flux distribution (see Figure 3-2) on the copper surface. Because of the nonuniformity, the mean flux to the copper surface was greater than 20.2 kW/m^2 used in the theoretical calculations (Eq. 4-15). Figure 4-4 demonstrates that Eq. 4-15 is in good agreement with experimental data.

4.2.2 Finite Depth Spills Transparent to Thermal Radiation

If the spill is fully transparent to the incident thermal flux, then the incident energy is delivered at the liquid-substrate interface (i.e., at x=d in Figure 4-3) rather than at the liquid-air interface. It is assumed that the net flux to the spill is due to thermal radiation alone and that no heat transfer occurs at the liquid-air interface (at x=0 in Figure 4-3). The energy equations for liquid and substrate are the same as in Section 4.2.1 (Eqs. 4-6 and 4-7 respectively). The (new) interface boundary conditions for the transparent case are:

$$- \lambda_2 \frac{\partial T_2}{\partial x}\bigg|_{x=d} + \lambda_1 \frac{\partial T_1}{\partial x}\bigg|_{x=d} = \dot{q}'' \qquad (4\text{-}17)$$

and (as in Section 4.2.1):

$$T_1(x=d) = T_2(x=d) \quad . \qquad (4\text{-}18)$$

The initial condition is (as in Section 4.2.1):

$$T_1 = T_2 = T_0 \quad \text{at} \quad t=0 \qquad (4\text{-}19)$$

where T_0 is the initial (ambient) temperature of the system.

The (new) boundary condition at the (insulated) liquid-air interface is:

$$- \lambda_1 \frac{\partial T_1}{\partial x}\bigg|_{x=0} = 0 \quad . \qquad (4\text{-}20)$$

The solution for the liquid spill temperature, $T_1(x,t)$, is obtained in a manner similar to that in Section 4.2.1 (Appendix B). It is given by:

$$T_1(x,t) - T_0 = \frac{2\dot{q}''}{\sqrt{\lambda_1 \rho_1 c_1}} \left(\frac{1}{1+m}\right) \sqrt{t} \sum_{n=0}^{\infty} \sigma^n \left\{ \text{ierfc} \left[\frac{(2n+1)d + x}{2\sqrt{\alpha_1 t}}\right] + \text{ierfc} \left[\frac{(2n+1)d - x}{2\sqrt{\alpha_1 t}}\right] \right\} \quad \text{for } 0 \leq x \leq d \quad . \tag{4-21}$$

The surface temperature rise, ΔT, is obtained by putting x=0 in Eq. 4-21:

$$\Delta T = \frac{4\dot{q}''}{\sqrt{\lambda_1 \rho_1 c_1}} \left(\frac{1}{1+m}\right) \sqrt{t} \sum_{n=0}^{\infty} \sigma^n \, \text{ierfc} \left[\frac{(2n+1)d}{2\sqrt{\alpha_1 t}}\right] \quad . \tag{4-22}$$

Not unexpectedly, Eq. 4-22 reduces to Eq. 4-16 for thin spills $\left(\frac{d}{\sqrt{\alpha_1 t}} \to 0\right)$. This implies that, for thin spills, both opaque as well as transparent models yield the same solution. This result is encouraging since unconfined spills of oil are, indeed, quite thin (see Table 3-4). Therefore, the opaque and the transparent models can provide meaningful upper and lower limits, respectively, for the surface temperature for thin spills. For thick spills, the transparent model is not a very meaningful model: Eq. 4-22 shows that for the thick case ΔT tends to zero. The semi-transparent, semi-infinite model in Section 4.1 is more suitable for thick spills.

4.2.3 Finite Depth Spills - Comparison of Theory and Experiment

Figure 4-5a shows a comparison of theory and experiment for a typical unconfined spill of finite depth, on a conducting substrate. The example shown in Figure 4-5a is that of an unconfined spill of Pennzoil 30-HD (depth 0.75 mm) on a steel substrate. The tungsten-quartz lamps were set at 13.8 kW/m^2. The solid line represents experimental measurements of oil surface temperature. The vertical bar is a measure of repeatability. The upper boundary of the shaded region represents the theoretical solution for an opaque spill (Eq. 4-15) and the lower boundary, the solution for a transparent spill (Eq. 4-22). Similar to the semi-infinite case (Figure 4-2a), the net flux $\dot{q}''$ in Eqs. 4-15 and 4-22 was estimated to be 10 kW/m^2 for a lamp setting of 13.8 kW/m^2. The two limiting solutions bracket the measured temperature response. Of the two solutions, the opaque solution (Eq. 4-15) is not only the more conservative one, but also the better approximation for exposure times exceeding about 300 s.

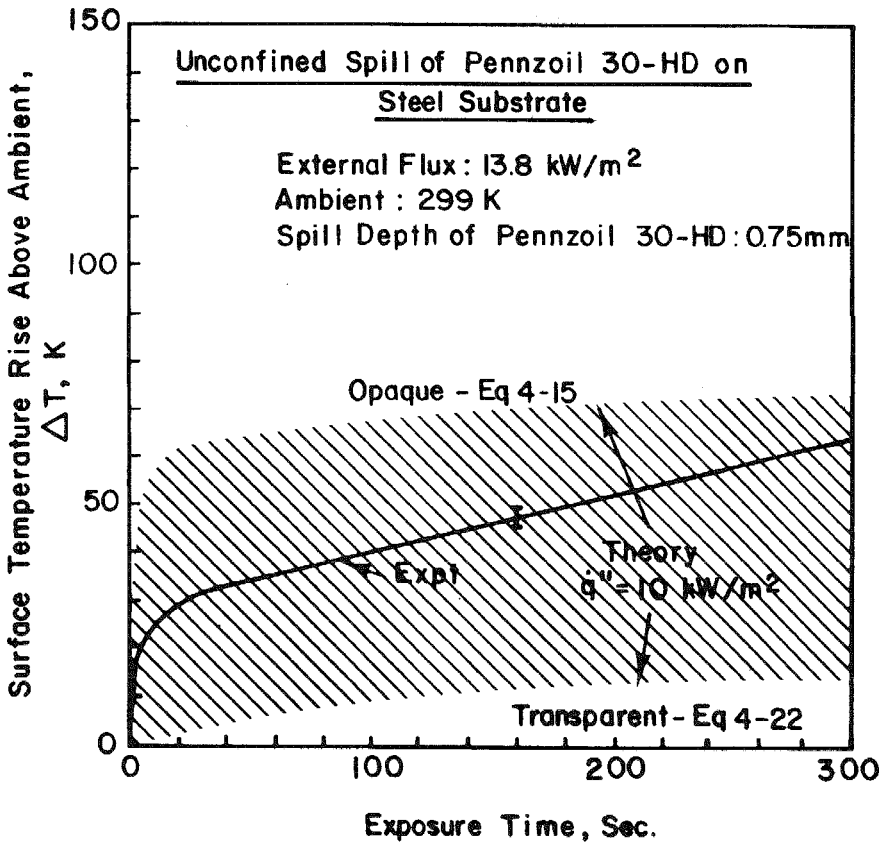

Figure 4-5a. A comparison of experiment (solid line) and the range (shaded region) predicted by two theoretical limits (opaque limit - eq 4-15; and fully transparent limit - eq 4-22) for an unconfined spill of Pennzoil 30-HD on a steel substrate. The vertical bar is a measure of test-to-test repeatability. Of the two limiting solutions, the opaque limit is more conservative and also the closer approximation to measurements for exposures exeeeding about 300 seconds.

A similar comparison is shown in Figure 4-5b for an epoxy-coated, concrete substrate. For exposure times exceeding 100 s, measured temperatures are somewhat higher than those predicted by Eq. 4-15 (opaque limit). This is possibly due to the unevenness of the concrete surface. As a result, it is likely that the local depth where the temperatures were measured was somewhat greater than 0.75 mm, resulting in higher surface temperatures.

Figures 4-5a and 4-5b indicate that, although Eq. 4-15 strictly applies only to opaque spills, it is a generally satisfactory approximation even for semi-transparent spills (of finite depth).

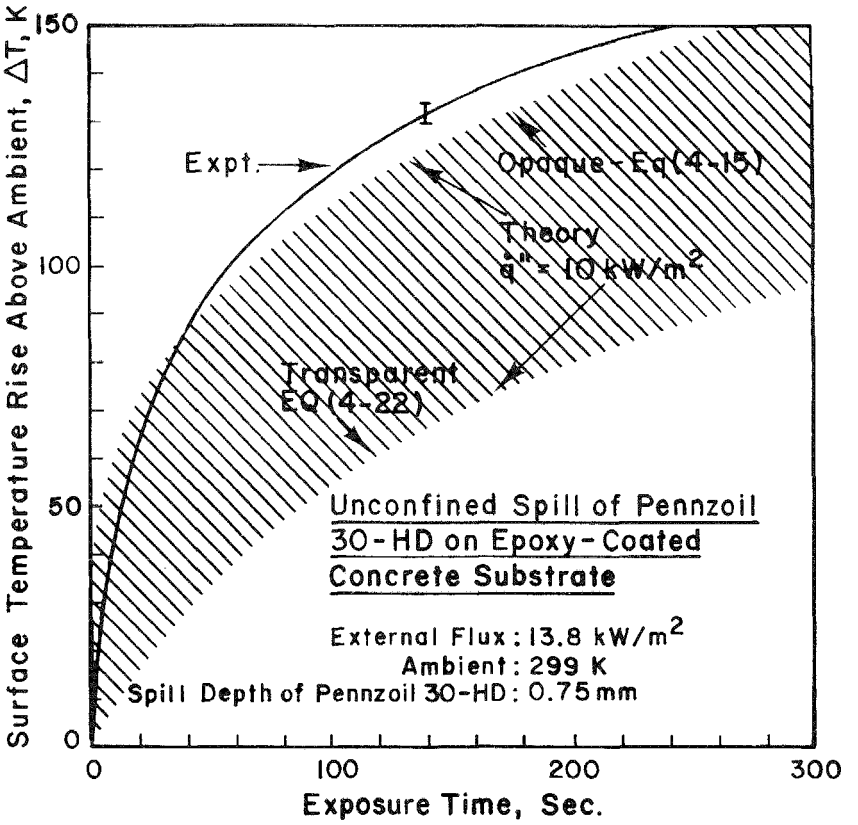

Figure 4-5b. Unconfined spill of Pennzoil 30-HD on an epoxy-coated concrete substrate.

Section 5
CONCLUDING REMARKS

Since full-scale tests are expensive and difficult to conduct in a controlled manner, here we have developed small-scale test methods and analytic formulae to determine the ignitability of high-fire-point flammable liquid spills as might occur in electric utility installations.

Several conclusions can be drawn from the results presented. The results indicate that confined spills, because they are usually deeper, present a greater fire hazard than unconfined spills. Because of the greater depth of the confined spill, less heat is conducted away by the surface over which the (confined) spill has occurred. The time to ignite a deep spill of a flammable liquid depends primarily on two factors: 1) the net energy flux to the surface of the spill, and 2) its fire point. The thermal radiation flux, in turn, depends on the environment in the vicinity of the spill. In the present program it was assumed that a spill is threatened by a source fire non-contiguous with the spill but adjacent to it. The top line in Figure 5-1 shows the total radiation flux (as a function of source fire diameter) from a typical hydrocarbon source fire (2,24) to a spill near the edge of the fire. Because of convective and radiative heat losses at the spill surface and attenuation of the incident radiation flux by the vapors issuing from the spill, the net flux to the spill surface is only about 65% of the total external flux. The net flux is shown by the bottom line of Figure 5-1. Figure 5-2 (see Eq. 4-4) shows the time to ignite deep spills versus net flux for two semi-transparent flammable liquids: a high-fire-point liquid (586 K; Fyrquel 220) and a low-fire-point liquid (402 K; #2 fuel oil). Figure 5-2 shows that ignition times decrease with increasing flux (i.e., with increasing size of the source fire; see Figure 5-1). Further, it takes longer to ignite a high-fire-point spill than a low-fire-point spill. The shaded region in Figure 5-2 shows the range of ignition times for common flammable liquids. This range of ignition times was found to agree reasonably with a large-scale experiment using a 1.2-m diam heptane source fire. In that experiment all the liquids tested ignited between 120 s and 260 s (see Table 2-1); Figures 5-1 and 5-2 indicate a range of 20 s to 400 s. Figures 5-1 and 5-2 show that it takes a long time ($>>$ 1000 s) to ignite a spill if the diameter of the source fire is less than 200 mm. However, for source fires larger than 200 mm, ignition times decrease rapidly with increasing fire size.

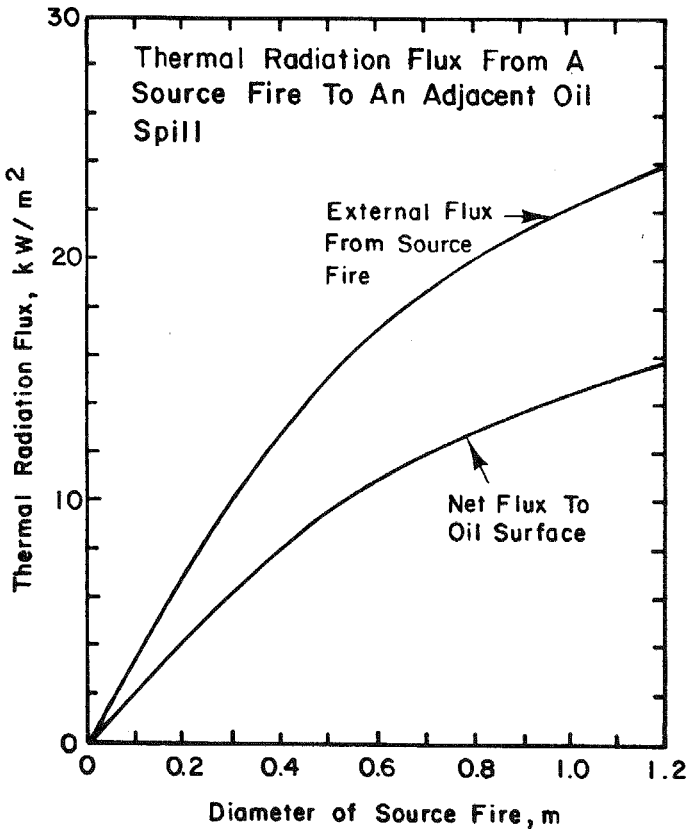

Figure 5-1. Thermal radiation flux from a typical hydrocarbon source fire to a spill non-contiguous with the fire but adjacent to it is shown as a function of source fire diameter. The top line shows the total flux from the source fire. The bottom line is an approximate estimate of the net flux to the spill surface accounting for convective and surface radiation losses at the spill surface and losses due to absorption of the incident radiation in the vapor plume above the spill surface. The net flux is assumed to be 65 percent of the total flux.

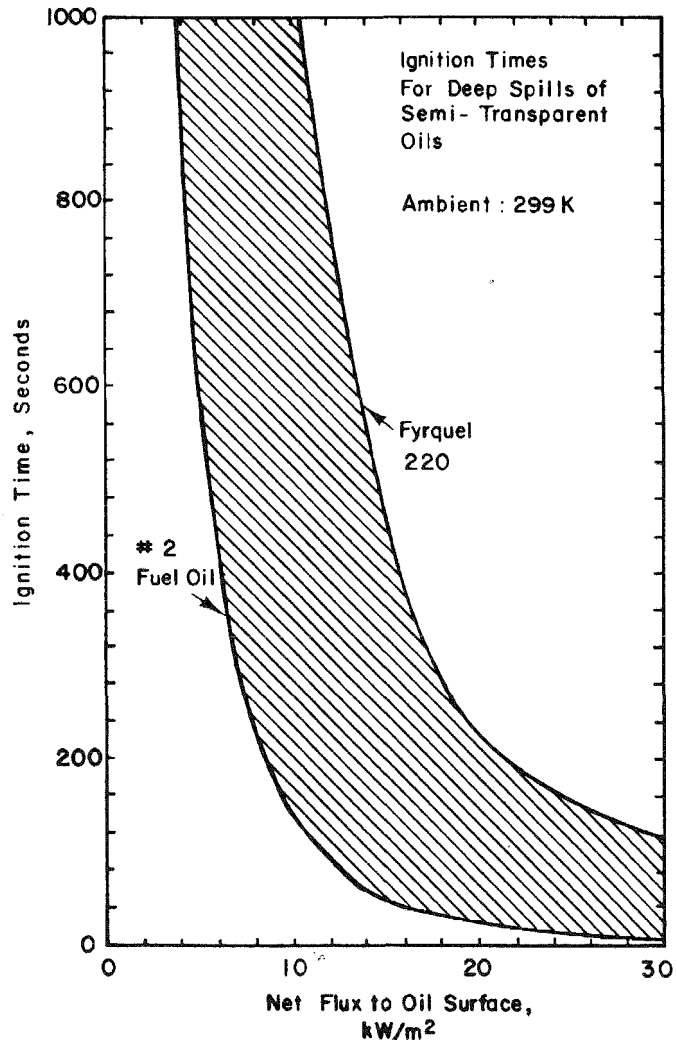

Figure 5-2. Ignition time (piloted) for deep spills of semi-transparent hydrocarbon liquids are shown as a function of the net radiant flux to the spill for a high fire point liquid (586 K; Fyrquel 220) and a relatively low fire point liquid (402 K, #2 fuel oil). The shaded region shows the range of ignition times for common hydrocarbon liquids. Ignition times decrease with increasing flux (i.e., with increasing size of the source fire). A low fire point spill ignites sooner than a high fire point spill.

Large-scale tests also show that, regardless of depth, it is not possible to ignite an oil spill by an exposure of less than 60 s to weld spatter. It is also not possible to ignite a spill by direct exposure of less than 15 s to an oxyacetylene welding torch.

An important, but not unexpected, phenomenon observed here was that the semi-transparency of a spill significantly affects its surface temperature response. This is especially true for confined (i.e., deep) spills and implies that, other factors being equal, contaminated spills (which are likely to be less transparent) will ignite sooner than uncontaminated spills. The ignition time for a confined and contaminated (opaque) spill is easily estimated from Eq. 4-5. In general, uncontaminated hydrocarbon liquids (except #6 residual oil which is opaque) are semi-transparent to infrared radiation. All hydrocarbon oils are semi-transparent to more or less the same extent. In addition, the thermal conductivities and volumetric heat capacities for all hydrocarbon oils are nearly the same (see Table 3-3). Therefore, the temperature response of all confined spills is similar. The temperature response for (deep) confined, semi-transparent spills is given by Eq 4-4.

The depth of an unconfined spill, is independent of spill volume and varies from oil to oil. This depth is a property of the liquid and, if the substrate is nonabsorbing, it is relatively independent of the substrate type over which the oil is spilled. Because the depth varies, the temperature response of an unconfined spill varies from oil to oil and depends on the thermal inertia of the substrate under the spill. The experimentally measured temperature response of a spill of finite depth can be reasonably well predicted by Eq. 4-15 for opaque as well as semi-transparent liquids.

In summary, seven noteworthy results emerge from this study:

1. Regardless of spill depth, it is not possible to ignite a spill by less than 60-s exposure to weld spatter or less than 15-s direct exposure to an oxyacetylene welding torch.
2. It takes a long time (>> 1000 s) to ignite a spill adjacent to a source fire if the source fire is less than 200 mm in diameter. However, ignition times decrease rapidly for source fires of diameter larger than 200 mm.
3. Infrared transmission and thermal properties of most hydrocarbon liquids are similar. Their fire points, however, can differ markedly.
4. Deep spills (depth > 20 mm) present a greater fire hazard than shallow spills.
5. Low-fire-point spills are more hazardous than high-fire-point spills.

6. If the floor of a utility installation is nonabsorbing, then the depth of an unconfined spill primarily depends on the oil and not the floor material. The depth of an unconfined spill on a truly horizontal surface is independent of the spill volume. Hydrocarbon oil spills show markedly differing depths of unconfined spills. These depths may vary by as much as a factor of 4 and they are all generally less than 1 mm deep. Because of markedly differing depths, the surface temperature response of unconfined spills varies from oil to oil. The temperature response of a shallow spill depends on the thermal properties of the floor.

7. The ignition time of a spill can be estimated reasonably well on the basis of the time to reach its fire point. The simple formulae developed here can provide satisfactory estimates of ignition times for deep as well as shallow spills of flammable liquids.

REFERENCES

1. J.S. Newman and J.P Hill. "Assessment of Exposure Fire Hazard to Cable Trays," Factory Mutual Research Corporation Technical Report FMRC J.I. 0C2R7.RC, RC80-T-56, July 1980.

2. A.T. Modak. Combustion and Flame. 29, 177 (1977).

3. A.T. Modak and P.A. Croce. Combustion and Flame. 30, 251 (1977).

4. A. Robert. Stone and Webster Engineering Corporation, Boston, personal communication, November 1979.

5. A. Tewarson, J.L. Lee and R.F. Pion. Eighteenth Symposium (International) on Combustion, The Combustion Institute, 1981, in press.

6. D.E. Gray, Editor, American Institute of Physics Handbook, McGraw-Hill, New York, 1957, p. 6-79, Table 6g-12.

7. T.Z. Harmathy. ASTM J. Mater. 5 (1), 47 (1970).

8. T.T. Lie and G. Williams-Leir. Fire and Materials, 3 (2), 74-79 (1979).

9. T.Z. Harmathy and L.W. Allen. ACI Journal, Title No 70-15, February 1973.

10. O.A. Hougen, K.M. Watson and R.A. Ragatz. Chemical Process Principles, Part I : Material and Energy Balances, 2nd Edition, Asia Publishing House, Bombay 1961, p. 42.

11. D.Q. Kern. Process Heat Transfer, Appendix of Calculation Data, McGraw-Hill, New York, 1950, pp 803, 806 and 809.

12. Anon. National Bureau of Standards, Misc. Pub. 97.

13. Anon. Brochure on Fyrquel, Fire Resistant Fluids and Lubricants, Stauffer Chemical Company, Specialty Chemical Division, Westport, Connecticut 06880, 1979.

14. Anon. "Selected Values of Properties of Hydrocarbons and Related Compounds; Category B: Infrared Spectral Data" 9 volumes: American Petroleum Institute, Thermodynamics Research Center Hydrocarbon Project 1977 (formerly API Research Project 44).

15. R.A. Matula and R.C. Farmer. "Combustion Kinetics of Selected Aromatic Hydrocarbons," Interim Report, College of Engineering, Louisiana State University, Baton Rouge, Louisiana, AFOSR-77-3384, June 1978.

16. T. Kashiwagi. Combustion Science and Technology 21, 131, 1980.

17. M.G. Velarde and C. Normand. "Convection," Scientific American, July 1980, pp. 92-108.

18. C. Normand, Y. Pomeau and M.G. Velarde. Reviews of Modern Physics, 49, (3) 581-624, July 1977.

19. J.C. Boehringer and R.J. Spindler. AIAA Journal 1 (1) 84-88, 1963.

20. H.S. Carslaw and J.C. Jaeger. Conduction of Heat in Solids, Clarendon Press, Oxford, 1959, 2nd edition, p. 32.

21. J. de Ris. Seventeenth Symposium (International) on Combustion, The Combustion Institute, Pittsburgh, 1979, p. 1003.

22. W.H. McAdams. Heat Transmission, McGraw-Hill, New York, 1954, p. 180.

23. M. Abramowitz, and I. Stegun. Handbook of Mathematical Function, NBS, Applied Mathematics Series 55, Washington, D.C., June 1964, p. 1026, Formula 29.3.85.

24. L. Orloff. "Simplified Radiation Modeling of Pool Fires," Eighteenth Symposium (International) on Combustion, Waterloo, Canada, 1980, (in press).

Appendix A

EFFECT OF THERMOCOUPLE SIZE ON SURFACE TEMPERATURE MEASUREMENTS

To establish whether meaningful measurements of surface temperatures of oil spills were possible, temperatures were measured with (chromel-alumel) thermocouples of different wire diameters and bead sizes. We measured the temperature-time response of the surface of a 120-mm deep pool of Pennzoil 30-HD mixed with 20% by volume of #1 Lampblack 228 83 mixture (Benjamin Moore and Co., Montvale, N.J. 07645). The thermocouple wires were made to lie flush with the oil surface and the thermocouple bead was made to float on the oil surface. The thermocouple assembly was adjusted so as to maintain a uniform meniscus. Uniformity of meniscus was determined visually.

Figure A-1 shows measurements made with a chromel-alumel thermocouple of 0.28 mm diam wires and a 0.76 mm diam bead size; and a fine wire thermocouple of 0.13-mm diam wires and a 0.13-mm diam bead size. The vertical bar in Figure A-1 indicates the test-to-test repeatability of the measurements.

Figure A-1 shows that measured temperatures are independent of thermocouple size.

Since it was easier to float the fine wire thermocouple, in the present program all temperature measurements of the oil surface were made with 0.13-mm diam wire, 0.13-mm diam bead size, chromel-alumel thermocouples.

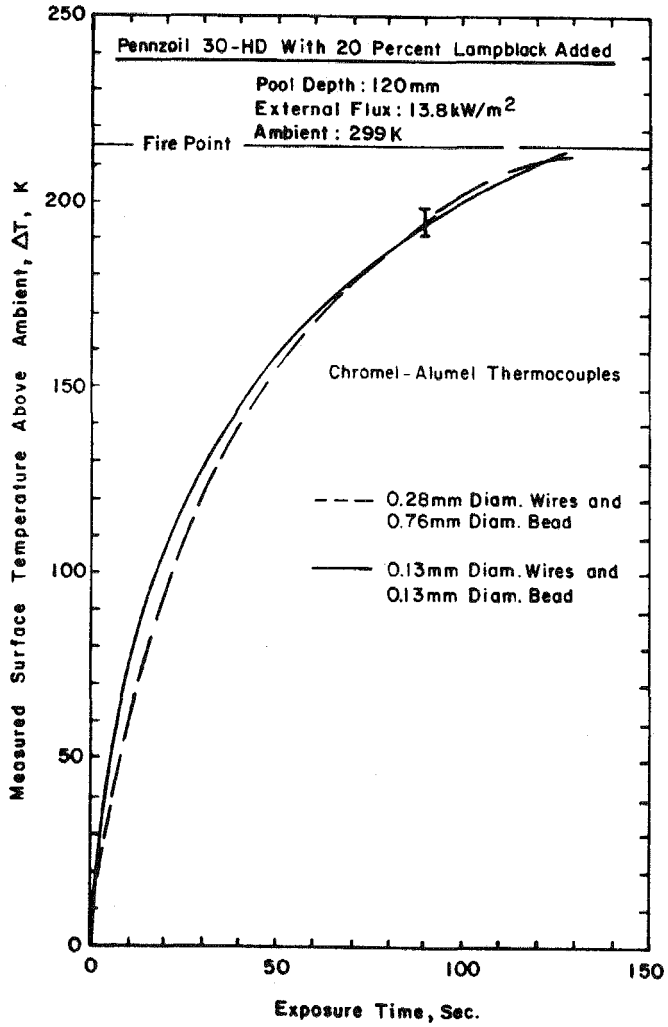

Figure A-1. Measured surface temperature rise above ambient versus time of exposure to 13.8 kW/m^2 radiant flux for a 120 mm deep pool of Pennzoil with 20 percent lampblack mixture added. Measurements were made with two chromel-alumel thermocouples of different sizes. Measurements with the larger size are shown by the dashed line. The solid line shows results with a fine wire thermocouple. Test-to-test repeatability of these measurements is shown by the vertical bar. Measured temperatures are independent of thermocouple size. All measurement reported in the present program were made with the fine wire thermocouple.

Appendix B

SOLUTION OF EQUATIONS 4-6 AND 4-7 BY LAPLACE TRANSFORMS

Let $\bar{\theta} = \int_{t=0}^{\infty} \theta e^{-st}\, dt$, the Laplace transform of θ

where

$$\theta = (T - T_0) \quad :$$

Then the transformed Eqs. 4-6 and 4-7 are

$$\frac{d^2\bar{\theta}1}{dx^2} - \frac{s}{\alpha_1}\bar{\theta}_1 = 0 \qquad 0 \leq x \leq d \tag{B-1}$$

and

$$\frac{d^2\bar{\theta}_2}{dx^2} - \frac{s}{\alpha_2}\bar{\theta}_2 = 0 \qquad d \leq x < \infty \quad . \tag{B-2}$$

OPAQUE SPILLS:

The transformed boundary conditions for opaque spills are:

$$\lambda_1 \frac{d\bar{\theta}_1}{dx}\bigg|_{x=d} = \lambda_2 \frac{d\bar{\theta}_2}{dx}\bigg|_{x=d} \tag{B-3}$$

$$\bar{\theta}_1\ (x=d) = \bar{\theta}_2\ (x=d) \tag{B-4}$$

and

$$-\lambda_1 \frac{d\bar{\theta}_1}{dx}\bigg|_{x=0} = \frac{\dot{q}''}{s} \tag{B-5}$$

The solution to (the ordinary differential) Eqs. B-1 and B-2 are:

$$\bar{\theta}_1 = A_1 e^{-\left(\frac{s}{\alpha_1}\right)^{1/2} x} + B_1 e^{\left(\frac{s}{\alpha_1}\right)^{1/2} x} \tag{B-6}$$

and

$$\bar{\theta}_2 = A_2 \, e^{-\left(\frac{s}{\alpha_2}\right)^{1/2} x} \tag{B-7}$$

The constants A_1, and B_1, (and A_2) are obtained by solving the three simultaneous Eqs. B-3, B-4, and B-5:

$$A_1 = \frac{\dot{q}''}{\sqrt{\lambda_1 \rho_1 c_1}} \cdot \frac{1}{s^{3/2}} \left[\frac{1}{1 - \sigma \, e^{-2\sqrt{s/\alpha_1}\, d}} \right] \tag{B-8}$$

and

$$B_1 = \frac{\dot{q}''}{\sqrt{\lambda_1 \rho_1 c_1}} \cdot \frac{1}{s^{3/2}} \left[\frac{\sigma \, e^{-2\sqrt{s/\alpha_1}\, d}}{1 - \sigma \, e^{-2\sqrt{s/\alpha_1}\, d}} \right] \tag{B-9}$$

The transformed temperature $\bar{\theta}_1$ in the liquid layer is then given by:

$$\bar{\theta}_1(x) = \frac{\dot{q}''}{\sqrt{\lambda_1 \rho_1 c_1}} \cdot \frac{1}{s^{3/2}} \cdot \left[\frac{e^{-\sqrt{s/\alpha_1}\, x} + \sigma \, e^{-\sqrt{s/\alpha_1}\, (2d-x)}}{1 - \sigma \, e^{-2\sqrt{s/\alpha_1}\, d}} \right] \tag{B-10}$$

The term $\left(1 - \sigma \, e^{-2\sqrt{s/\alpha_1}\, d}\right)$ in Eq. B-10 can be expanded in a binomial series:

$$\frac{1}{1 - \sigma \, e^{-2\sqrt{s/\alpha_1}\, d}} = 1 + \sum_{n=1}^{\infty} \sigma^n \, e^{-2\sqrt{s/\alpha_1}\, nd} \tag{B-11}$$

where $\sigma^2 \, e^{-4\sqrt{s/\alpha_1}\, d} < 1$.

Substituting Eq. B-11 in Eq. B-10 yields:

$$\bar{\theta}_1(x) = \frac{\dot{q}''}{\sqrt{\lambda_1 \rho_1 c_1}} \cdot \frac{1}{s^{3/2}} \left\{ e^{-\sqrt{s/\alpha_1}\, x} + \sum_{n=1}^{\infty} \sigma^n \left[e^{-\sqrt{s/\alpha_1}\, (2nd+x)} + e^{-\sqrt{s/\alpha_1}\, (2nd-x)} \right] \right\} \tag{B-12}$$

The inverse Laplace transform of Eq. B-12 is tabulated in Abramowitz and Stegun [23]:

$$T_1(x,t) - T_0 = 2\dot{q}'' \left(\frac{t}{\gamma_1\rho_1 c_1}\right)^{1/2} \left\{ \text{ierfc}\left(\frac{x}{2\sqrt{\alpha_1 t}}\right) + \sum_{n=1}^{\infty} \sigma^n \left[\text{ierfc}\left(\frac{2nd+x}{2\sqrt{\alpha_1 t}}\right) + \text{ierfc}\left(\frac{2nd-x}{2\sqrt{\alpha_1 t}}\right) \right] \right\} \qquad \text{for } 0 \le x \le d \quad . \tag{B-13}$$

TRANSPARENT SPILLS

The transformed boundary conditions for transparent spills are:

$$-\lambda_2 \frac{d\bar{\theta}_2}{dx}\bigg|_{x=d} + \lambda_1 \frac{d\bar{\theta}_1}{dx}\bigg|_{x=d} = \frac{\dot{q}''}{s} \tag{B-14}$$

$$\bar{\theta}_1(x=d) = \bar{\theta}_2\ (x=d) \tag{B-15}$$

and

$$-\lambda_1 \frac{d\bar{\theta}_1}{dx}\bigg|_{x=0} = 0 \quad . \tag{B-16}$$

The transformed solution $\bar{\theta}_1(x)$ is given by:

$$\bar{\theta}_1(x) = \frac{\dot{q}''}{\sqrt{\lambda_1\rho_1 c_1}} \left(\frac{1}{1+m}\right) \cdot \frac{1}{s^{3/2}} \sum_{n=0}^{\infty} \sigma^n \left\{ e^{-\sqrt{s/\alpha_1}\,[(2n+1)d + x]} + e^{-\sqrt{s/\alpha_1}\,[(2n+1)d - x]} \right\} . \tag{B-17}$$

The inverse Laplace transform of Eq. B-17 is given [23] by:

$$T_1(x,t) - T_0 = \frac{2\dot{q}''}{\sqrt{\lambda_1\rho_1 c_1}} \cdot \frac{1}{1+m} \cdot \sqrt{t} \sum_{n=0}^{\infty} \sigma^n \left\{ \text{ierfc}\left[\frac{(2n+1)d + x}{2\sqrt{\alpha_1 t}}\right] + \text{ierfc}\left[\frac{(2n+1)d - x}{2\sqrt{\alpha_1 t}}\right] \right\} \qquad \text{for } 0 \le x \le d \quad . \tag{B-18}$$